Astron. Astrophys. 125, 150–167 (1983)

ASTRONOMY AND ASTROPHYSICS

DE 102: a numerically integrated ephemeris of the Moon and planets spanning forty-four centuries

X X Newhall, E. M. Standish, Jr., and J. G. Williams

Jet Propulsion Laboratory, California Institute of Technology, Pasadena, CA 91109, USA

Received October 15, 1982; accepted February 15, 1983

Summary. An ephemeris of the Moon and nine planets has been numerically integrated from 1411 BC to 3002 AD. The initial conditions for the simultaneous integration were based on fits to modern position measurements of the eight major planets and the Moon. The data include optical meridian transits, radar ranges, planetary spacecraft positions, and lunar laser ranges. The acceleration model for the integration is described and it is shown that the stability of the lunar integration depends upon simultaneously integrating the physical librations. A long ephemeris has utility for comparison with both historical observations and analytical theories. Comparison with numerical representations permits the equinox and obliquity of the ephemeris to be recovered. At B1950.0 we find $\varepsilon = 23°26'44''.816 \pm 0''.015$, which is $0''.039$ smaller than the presently adopted IAU value. Among the other determined parameters are the length of the astronomical unit, 149, 597, 870.68 ± 0.03 km. As newer, short ephemerides will continue to improve upon the accuracy of DE 102, analytical corrections can be provided over the long span of DE 102.

Key words: ephemerides

I. Introduction

The 1960's were a turning point for the generation of lunar and planetary ephemerides. All previous measurements of the positions of solar system bodies were optical angular measurements. Useful radar ranges to the surfaces of the terrestrial planets have been measured since 1964. The first laser ranges to the lunar corner cube retroreflectors were obtained in 1969. In 1976 the Viking landers on Mars began returning ranges with accuracies better than 10 m. In a relatively short time the transition from optical angles to Viking ranges improved the accuracy of Mars positions by more than four orders of magnitude, and the change from lunar angular measurements to laser ranges achieved nearly as great an improvement. These immense changes in observational accuracy due to modern technology have driven comparable improvements in the accuracy of the planetary and lunar ephemerides. While the fitting of optical data was long accomplished with analytical theories for the Moon and planets, the newer data types required the development of numerical integration techniques and more comprehensive physical models. The numerical integrations are necessary to match the accuracy of the modern data types. They are commonly extended back a few decades or centuries to allow the inclusion of the more recent optical data in the fits. We announce here the first integrated ephemeris, DE 102, which covers the entire span of the historical astronomical observations of usable accuracy which are known to us. The fit is made to modern data. The integration spans 1411 BC to 3002 AD.

The first use of a long integration is for comparisons with historical observations. In addition to the fruitful historical work that has been performed with analytical theories, we note that there are historical observations of fine accuracy which can usefully be linked with modern data types. Among these observations are the transits of the sun by Mercury as studied by Morrison and Ward (1975) and Shapiro (1980), and solar eclipses, of which the subset of Muller (1975) and Muller and Stephenson (1975) and the well observed 1715 eclipse (Dunham et al., 1980) are particularly useful. Linking historical optical data to modern ephemerides will provide valuable information on the irregularities in the earth's rotation at long time scales. DE 102 has estimated errors in the motions of the earth and Mars of $0''.04\ \mathrm{cy}^{-1}$ (cy = century) with respect to an inertial frame. Venus, Mercury, and the outer planets have progressively larger errors. The Moon has a quadratically growing error of up to $1''.2\ \mathrm{cy}^{-2}$ in longitude.

The second use of a long integration is for comparisons with analytical theories. Such comparisons serve two purposes: they provide a check on the solutions of the equations of motion, and they provide a means of adjusting the independent constants of the theories to the accurate fits to the modern data types. Long integrations are a valuable check because the long period terms are frequently the most troublesome in analytical solutions. One of the early motivations for this project was the discovery that solar eclipse data are sensitive to the lunar node rate, which has a poor value in the $j=2$ lunar theory (Martin and Van Flandern, 1970; Muller, 1975; Muller and Stephenson, 1975). It is gratifying that DE 102 has already been compared with Newcomb's theory of the earth's orbit (Van Flandern, 1982), a modified Newcomb's theory (Stumpff, 1981), Tuckerman's tables (Stephenson and Houlden, 1981), and a new theory for the earth (Bretagnon and Chapront, 1981). Such comparisons permit the recovery of the equinox offset and obliquity of DE 102. A theory for Mercury's orbit has been compared with the DE 102 orbit by Lestrade (1981) and Lestrade and Bretagnon (1982). The lunar orbit in DE 102 can be separately referred to as LE 51. It has been compared with a modified $j=2$ lunar ephemeris (Van Flandern, 1982) and a new lunar orbit theory (Chapront and Chapront-Touzé, 1981–1983).

Send offprint requests to: X X Newhall

Because of their expense, long integrations of the solar system are rare. The integration of this paper used nine days of computer time on a Univac 1100/81 and took six million steps. The 300,000-year integration of the five outer planets (Cohen et al., 1967) had a step size two orders of magnitude larger and took three million steps.

In this paper, Sects. II–IV describe the mathematical model used for the numerical integration of DE 102; the numerical integration program itself, including estimates of its accuracy; and the numerical representation of the resulting coordinates. Sections V–VII give the choices of the adopted constants, the observational data used in the least squares fits, and the least squares solutions themselves. Section VIII presents methods for modifying DE 102 in order to improve the approximation to more recent ephemerides. Comparisons of DE 102 with the latest (1981) JPL ephemeris are given in Sect. IX. Section X describes the export procedure for use by outside requestors.

II. Mathematical model

The dynamical evolution of the solar system throughout the span of the ephemeris was obtained from a simultaneous numerical integration of the equations of motion for the nine planets, the Moon and the lunar physical librations. The mathematical model includes contributions from (A) point-mass interactions, (B) figure effects, (C) earth tides, and (D) lunar librations. Each will be discussed in turn.

A. Point-mass interactions

The principal gravitational force on the nine planets, the sun, and the Moon is modeled by considering those bodies to be point masses in the isotropic, Parameterized Post-Newtonian (PPN) n-body metric (Will, 1974) with Newtonian gravitational perturbations from the asteroids (1) Ceres, (2) Pallas, (4) Vesta, (7) Iris, and (324) Bamberga. These were the five asteroids found to have the most pronounced effect on the Earth-Mars range in an integration from the standard 1969 epoch of initial conditions to 1985. The n-body equations were derived from the variation of a time-independent Lagrangian action integral formulated in a nonrotating solar-system barycentric Cartesian coordinate frame. The reference plane is the Earth's mean equator of B 1950.0. The x-axis coincides with neither the dynamical equinox nor the equinox of the FK 4 catalogue. In the DE 102 system the right ascension of the FK 4 equinox is about $+0''.40$; the right ascension of the dynamical equinox, defined in the rotating sense, is $-0''.136$ (Standish, 1982).

For each body i, the point-mass acceleration is given by

$$\ddot{\boldsymbol{r}}_{i_{\text{point mass}}} = \sum_{j\neq i}\frac{\mu_j(\boldsymbol{r}_j-\boldsymbol{r}_i)}{r_{ij}^3}\left\{1-\frac{2(\beta+\gamma)}{c^2}\sum_{k\neq i}\frac{\mu_k}{r_{ik}}-\frac{2\beta-1}{c^2}\sum_{k\neq j}\frac{\mu_k}{r_{jk}}+\gamma\left(\frac{v_i}{c}\right)^2+(1+\gamma)\left(\frac{v_j}{c}\right)^2\right.$$
$$\left.-\frac{2(1+\gamma)}{c^2}\dot{\boldsymbol{r}}_i\cdot\dot{\boldsymbol{r}}_j-\frac{3}{2c^2}\left[\frac{(\boldsymbol{r}_i-\boldsymbol{r}_j)\cdot\dot{\boldsymbol{r}}_j}{r_{ij}}\right]^2+\frac{1}{2c^2}(\boldsymbol{r}_j-\boldsymbol{r}_i)\cdot\ddot{\boldsymbol{r}}_j\right\}+\frac{1}{c^2}\sum_{j\neq i}\frac{\mu_j}{r_{ij}^3}\{[\boldsymbol{r}_i-\boldsymbol{r}_j]\cdot[(2+2\gamma)\dot{\boldsymbol{r}}_i-(1+2\gamma)\dot{\boldsymbol{r}}_j]\}(\dot{\boldsymbol{r}}_i-\dot{\boldsymbol{r}}_j)$$
$$+\frac{3+4\gamma}{2c^2}\sum_{j\neq i}\frac{\mu_j\ddot{\boldsymbol{r}}_j}{r_{ij}}+\sum_{m=1}^{5}\frac{\mu_m(\boldsymbol{r}_m-\boldsymbol{r}_i)}{r_{im}^3}, \tag{1}$$

where $\boldsymbol{r}_i$, $\dot{\boldsymbol{r}}_i$, $\ddot{\boldsymbol{r}}_i$ are the solar-system barycentric position, velocity, and acceleration vectors of body i; $\mu_j=Gm_j$, where G is the gravitational constant and m_j is the mass of body j; $r_{ij}=|\boldsymbol{r}_j-\boldsymbol{r}_i|$; β is the PPN parameter measuring the nonlinearity in superposition of gravity; γ is the PPN parameter measuring space curvature produced by unit rest mass (In this integration, as in general relativity, $\beta=\gamma=1$.); $v_i=|\dot{\boldsymbol{r}}_i|$; and c is the velocity of light.

In the last term on the right side of (1), quantities employing the index m refer to the asteroids. The positions of the asteroids are not integrated but are obtained from polynomials representing heliocentric Keplerian ellipses. The polynomials give good representations for perturbations on the planets at the present time. At times in the distant past the polynomials will drift from the real asteroid orbits, but the perturbations are smaller ($0''.02$ for Mars) than any ancient optical measurement accuracy.

The quantity $\ddot{\boldsymbol{r}}_j$ appearing in two terms on the right side of (1) denotes the barycentric acceleration of each body j due to Newtonian effects of the remaining bodies and the asteroids.

B. Figure effects

Long-term accuracy of the integrated lunar orbit requires the inclusion of the figures of the earth and Moon in the mathematical model. In DE 102 the gravitational effects due to figures include:

1. The force of attraction between the zonal harmonics (through fourth degree) of the earth and the point-mass Moon and Sun.

2. The force of attraction between the zonal harmonics (through fourth degree) and the second- and third-degree tesseral harmonics of the Moon and the point-mass Earth and Sun.

The mutual interaction between the figures of the Earth and Moon is ignored.

The contribution to the inertial acceleration of an extended body arising from the interaction of its own figure with an external point mass is expressed in the $\xi\eta\zeta$ coordinate system, where the ξ-axis is directed outward from the extended body to the point mass; the η-axis is directed east (lying in the selenographic xy-plane, perpendicular to the ξ-axis); and the ζ-axis is directed north, completing the right-hand system (see Fig. 1). In that system (Moyer, 1971),

$$\begin{bmatrix}\ddot{\xi}\\ \ddot{\eta}\\ \ddot{\zeta}\end{bmatrix}=-\frac{\mu}{r^2}\left\{\sum_{n=1}^{n_1}J_n\left(\frac{a}{r}\right)^n\begin{bmatrix}(n+1)P_n(\sin\phi)\\ 0\\ -\cos\theta P_n'(\sin\phi)\end{bmatrix}+\sum_{n=1}^{n_2}\left(\frac{a}{r}\right)^n\sum_{m=1}^{n}\begin{bmatrix}-(n+1)P_n^m(\sin\phi)[C_{nm}\cos m\lambda+S_{nm}\sin m\lambda]\\ m\sec\phi\,P_n^m(\sin\phi)[-C_{nm}\sin m\lambda+S_{nm}\cos m\lambda]\\ \cos\phi\,P_n'^m(\sin\phi)[C_{nm}\cos m\lambda+S_{nm}\sin m\lambda]\end{bmatrix}\right\}, \tag{2}$$

where μ is the gravitational constant G times the mass of the point body; r is the center-of-mass separation between the two bodies; n_1 and n_2 are the maximum degrees of the zonal and tesseral expansions, respectively; $P_n(\sin\phi)$ is the Legendre polynomial of degree n; $P_n^m(\sin\phi)$ is the associated Legendre function of degree n and order m; J_n are the zonal harmonics for the extended body; C_{nm}, S_{nm} are the tesseral harmonics for the extended body; a is the equatorial radius of the extended body; ϕ is the latitude of the

point mass relative to the body-fixed coordinate system in which the harmonics are expressed; λ is the east longitude of the point mass in the same body-fixed coordinate system.

The primes denote differentiation with respect to the argument $\sin\phi$.

The accelerations are transformed into the solar system barycentric Cartesian system by application of appropriate rotation matrices: first by a rotation from the $\xi\eta\zeta$ system to the selenographic system, followed by the application of the inverse libration-angle matrix.

The interaction between the figure of an extended body and a point mass also induces an inertial acceleration of the point mass. If $\ddot{r}_{\text{Fig}}$ denotes the acceleration given in Eq. (2) when expressed in solar system barycentric coordinates, then the corresponding acceleration $\ddot{r}_{\text{PM}}$ of the point mass is

$$\ddot{r}_{\text{PM}} = -\frac{\mu_{\text{Fig}}}{\mu_{\text{PM}}}\ddot{r}_{\text{Fig}}$$

where μ_{Fig} and μ_{PM} are the gravitation constant G times the masses of the extended body and point mass, respectively.

C. Earth tides

The tides raised by the Moon on the Earth appear as a bulge leading the Earth-Moon line by a phase angle δ. The resulting geocentric acceleration of the Moon is given by the expansion

$$\ddot{r}_{\text{tides}} = -\frac{3k_2\mu_m}{r_{em}^3}\left(1+\frac{\mu_m}{\mu_e}\right)\left(\frac{a_e}{r_{em}}\right)^5\begin{bmatrix} x+y\delta \\ y-x\delta \\ z \end{bmatrix},$$

where k_2 is the potential Love number of the earth; a_e is the radius of the earth; r_{em} is the geocentric lunar distance; x, y, z are the geocentric Cartesian coordinates of the Moon expressed in the true of-date system [The rotation to mean equator and equinox of B 1950.0 is performed by the application of an inverse nutation matrix followed by an inverse precession matrix. The nutation matrix is evaluated using only the leading (18.6 yr) term.]; μ_m is the gravitation constant times the mass of the Moon; μ_e is the gravitation constant times the mass of the Earth.

The inertial accelerations follow from the conservation of the center of mass. For further discussion, see Williams et al. (1978).

D. Lunar librations

A previous attempt at a long-term solar system integration yielded a secular runoff in lunar orbital longitude. The problem was traced to the use of an analytical theory for the computation of lunar librations, acting as a forcing function for the system through figure perturbations. When the differential equations for the physical librations were implemented and integrated, the secular instability disappeared.

It was necessary to form a matrix transforming between the coordinates with a fixed equator and equinox of B 1950.0 and the selenographic system. The Euler angle definitions and their differential equations were taken from Goldstein (1950). ϕ is the angle along the earth's fixed equator from the fixed equinox to the line of nodes with the Moon's true equator; θ is the inclination of the Moon's true equator to the earth's fixed equator; and ψ is the angle along the Moon's equator from the line of nodes to the reference meridian of the selenographic system. Following customary procedures, we define

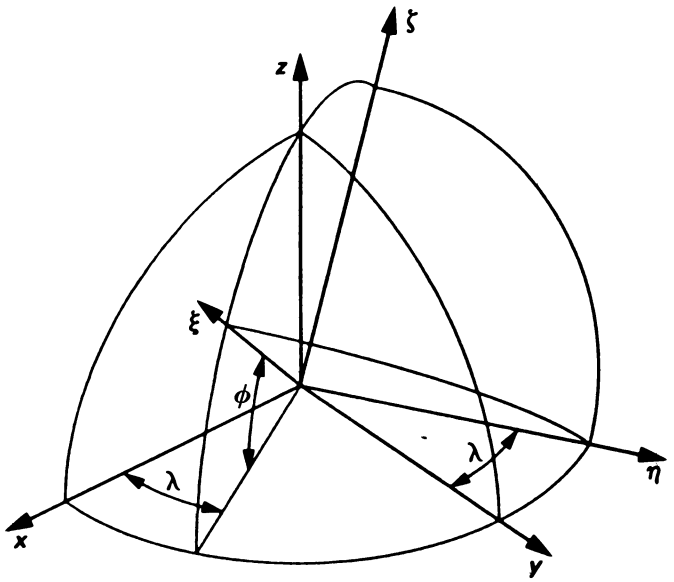

Fig. 1. The $\xi\eta\zeta$ coordinate system, in which figure-induced accelerations are calculated

$$\beta_L \equiv \frac{C-A}{B}$$

and

$$\gamma_L \equiv \frac{B-A}{C}$$

where A, B, and C are the three principal moments of inertia of the Moon, and $C>B>A$. The relationship between β_L, γ_L, J_2, C_{22}, and C/ma^2 (where m is the mass of the Moon and a is the lunar radius) is described in Ferrari et al. (1980).

Let $\boldsymbol{F}_{\text{Fig}}$ be the force on the Moon due to the gravitational interaction of the lunar figure and an external point-mass earth or sun. $\boldsymbol{F}_{\text{Fig}}$ is derived from Eq. (2). Then the torque $\boldsymbol{N}$ on the Moon is given by

$$\boldsymbol{N} = \boldsymbol{r} \times \boldsymbol{F}_{\text{Fig}}$$

where $\boldsymbol{r}$ is the vector from the lunar center of mass to the point mass. In the selenographic principal-axis system the equations for the angular velocity vector $\boldsymbol{\omega}$ are related to the Euler angles through

$$\omega_x = \dot{\phi}\sin\theta\sin\psi + \dot{\theta}\cos\psi$$

$$\omega_y = \dot{\phi}\sin\theta\cos\psi - \dot{\theta}\sin\psi$$

$$\omega_z = \dot{\phi}\cos\theta + \dot{\psi}.$$

The differential equations for the angular velocity come from Euler's equations

$$\dot{\omega}_x = \frac{\gamma_L-\beta_L}{1-\beta_L\gamma_L}\omega_y\omega_z + \frac{N_x}{A}$$

$$\dot{\omega}_y = \beta_L\omega_z\omega_x + \frac{N_y}{B}$$

$$\dot{\omega}_z = -\gamma_L\omega_x\omega_y + \frac{N_z}{C}.$$

Finally, the differential equations for the three Euler angles are

$$\ddot{\phi}=\frac{\dot{\omega}_x\sin\psi+\dot{\omega}_y\cos\psi+\dot{\theta}(\dot{\psi}-\dot{\phi}\cos\theta)}{\sin\theta}$$

$$\ddot{\theta}=\dot{\omega}_x\cos\psi-\dot{\omega}_y\sin\psi-\dot{\phi}\dot{\psi}\sin\theta \tag{3}$$

$$\ddot{\psi}=\dot{\omega}_z-\ddot{\phi}\cos\theta+\dot{\phi}\dot{\theta}\sin\theta.$$

The above second-order differential equations for the Euler angles of a rigid body Moon are integrated numerically, considering torques induced by the Earth and Sun.

Discussions of numerically integrated physical librations are given by Williams et al. (1973) and Cappallo (1980, 1981). Nonrigid-body effects are described by Yoder (1978) and Cappallo (1980). The numerically integrated physical librations used to fit the lunar laser data came from the program described by Williams et al. (1973) rather than from the program described here.

E. Solar system barycenter

In the n-body metric, all dynamical quantities are expressed with respect to a center of mass whose definition is modified from the usual Newtonian formulation. The solar system barycenter is given by (Estabrook, 1971, private communication):

$$\sum_i \mu_i^* \boldsymbol{r}_i=\boldsymbol{0}, \tag{4}$$

where

$$\mu_i^*=\mu_i\left\{1+\frac{1}{2c^2}v_i^2-\frac{1}{2c^2}\sum_{j\neq i}\frac{\mu_j}{r_{ij}}\right\}. \tag{5}$$

In (5),

μ_i is defined as before

v_i is the barycentric speed of body i

$r_{ij}=|\boldsymbol{r}_j-\boldsymbol{r}_i|$.

During the process of numerical integration only the equations of motion for the Moon and planets were actually evaluated and integrated. The barycentric position and velocity of the sun were obtained from (4). It should be noted that each of Eqs. (4) and (5) depends on the other, requiring an iteration during the evaluation of the solar position and velocity.

III. Numerical integration

The numerical integration of the equations of motion (1) and (3) was carried out using a variable step-size, variable-order Adams method (Krogh, 1972). The maximum allowable order of any of the thirty-three equations is 14; the actual order at any instant is determined by a specified error bound and by the behavior of backward differences of accelerations.

A. Force model evaluation

The calculation and arrangement of accelerations at each integration step is as follows:

1. The integrator subroutine provides new states (positions and velocities) for the nine planets, the Moon, and the libration angles.

2. The asteroid states are evaluated from fixed polynomials.

3. Equations (5) for the relativistic masses are evaluated for the planets, Moon, asteroids, and sun, using current states for all bodies except the Sun. (The barycentric state of the sun calculated at the end of the previous step is retained for this evaluation.)

4. The present approximate state of the sun is obtained from the constraint Eq. (4).

5. Equations (5) are evaluated again, using this new estimate of the solar state.

6. Equation (4) is evaluated a second time to provide the current state of the Sun.

7. Equations (1) are evaluated to obtain the accelerations of the nine planets and the Moon.

8. It has proved numerically more suitable to integrate the lunar ephemeris relative to the earth rather than to the solar system barycenter. The solar system barycentric Earth and Moon states are replaced by the quantities $\boldsymbol{r}_{em}$ and $\boldsymbol{r}_B$, given by

$$\boldsymbol{r}_{em}=\boldsymbol{r}_m-\boldsymbol{r}_e \tag{6}$$

and

$$\boldsymbol{r}_B=\frac{\mu_e\boldsymbol{r}_e+\mu_m\boldsymbol{r}_m}{\mu_e+\mu_m}, \tag{7}$$

where the subscripts e and m denote the Earth and Moon, respectively. Note that $\boldsymbol{r}_{em}$ is the difference of solar system barycentric vectors and is distinguished from a geocentric vector by the relativistic transformation from the barycenter to geocenter. (The vector $\boldsymbol{r}_B$ can be interpreted as representing the coordinates of the Newtonian Earth-Moon barycenter relative to the solar system barycenter. It has no physical significance and does not appear in force calculations; it is solely a vehicle for improving the numerical behavior of the differential equations.)

9. The equations for the libration angle accelerations are evaluated.

B. Estimated integration error

The method of error control used in the integration puts a limit on the absolute value of the estimated error in velocity of each equation at the end of every integration step. Step size and integration orders are adjusted on the basis of estimated error. The limits selected for DE 102 are $2\,10^{-16}$ au d^{-1} in each component of the equations of motion for the planets and Moon, and $2\,10^{-14}$ rad d^{-1} for each component of the libration equations.

The effects of error control are most pronounced in the lunar ephemeris. For comparison, a twenty-year integration with the DE 102 initial conditions was performed with the absolute error tolerances decreased by a factor of ten. The geocentric lunar distance, latitude, and longitude were compared. The latitude showed no significant difference. The longitude difference exhibited a secular, exponential-like drift, comfortably fit by the expression

$$r\Delta\lambda=-10^{-9}t^{1.7}\,\text{km},$$

where $r\Delta\lambda$ is the standard lunar position minus the position from the comparison integration, projected onto the direction of increasing longitude, and t is the time in days from the start of the integration (JED 2440400.5). Extrapolating this formula, the longitudes will differ by about one meter after ten years, a kilometer after 500 yr, and by about 23 km at the earliest epoch (1411 BC) achieved by the integration. For comparison, the

uncertainty in the lunar longitude due to uncertainties in the secular acceleration is one to two orders of magnitude larger.

The difference in the radial direction shows an uneven oscillation about zero. The oscillation has an envelope given approximately by the expression $5\,10^{-11}\,t^{1.7}$, in kilometers. As this is smaller than the longitude difference by a factor of the lunar eccentricity, it is clear that it is just the mean anomaly runoff showing in the radius.

Similar comparisons for Mercury are a factor of ten less than those for the Moon; differences for the remaining planets and for the librations are negligibly small.

It should be stressed that such an empirically derived estimate is at best qualitative and indeed may be unduly pessimistic. More reliably quantitative analyses of the numerical behavior of the integration process are not so easily undertaken.

C. *Stability of the lunar integration*

Our first long integration (DE 97/LE 47) generated a lunar ephemeris which was adequate to fit the lunar ranges but deviated considerably in orbital longitude after three centuries when compared to the analytical lunar theory (Van Flandern, 1977, private communication). This unexpected situation was traced to the modeling of the orientation of the lunar body in the integration and the resultant accelerations due to the lunar gravitational harmonics. The difficulty was not mistaken programming but rather an instability in the equations of motion of the orbit which arises if the physical librations are modeled analytically. Related difficulties have appeared in the literature, and it seems worthwhile to present calculations illustrating the instability.

Consider first the expression for the disturbing function due to lunar gravitational harmonics $C_{\ell m}$ and $S_{\ell m}$ (Kaula, 1966), where $\ell - m$ is even

$$R_{\ell m} = \frac{\mu}{a}\left(\frac{a_m}{a}\right)^{\ell} \sum_p F_{\ell m p}(i) \sum_q G_{\ell p q}(e) \cdot \{C_{\ell m}\cos[(\ell-2p)\omega + (\ell-2p+q)M + m(\Omega-\theta)] + S_{\ell m}\sin[(\ell-2p)\omega + (\ell-2p+q)M + m(\Omega-\theta)]\}, \quad (8)$$

where a_m is the equatorial radius of the Moon and a, e, i, Ω, ω, and M are the osculating Keplerian elements (semimajor axis, eccentricity, inclination, node, argument of perifocus, and mean anomaly) of the orbit of the Moon about the Earth. The orientation angles i, Ω, and ω are referred to the instantaneous lunar equator. In this expression for perturbations of the relative Earth-Moon orbit, μ is the gravitational constant times the sum of the masses of the Earth and Moon. The angle θ describes the angle of rotation of the lunar zero meridian from the vernal equinox. The functions F and G are given by Kaula.

Let us examine the simplest case needed to illustrate our runoff. We restrict this exposition to the second degree terms ($\ell = 2$) for a triaxial Moon, C_{20} and C_{22}, with the major axis in the mean direction of the earth ($S_{22} = 0$). The instability arises from the physical libration terms in longitude, so the latitude terms will be ignored and i will now be taken to be the mean inclination of the lunar orbit to the lunar equator. Since θ has the same mean rate as $M + \omega + \Omega$, we retain only the slow terms by setting $2 - 2p + q = m$. Further, since the C_{20} term is independent of θ, only the C_{22} terms are retained. With these restrictions the one component of the disturbing function becomes

$$R_{22} = \frac{3\mu C_{22} a_m^2}{2a^3}(1+\cos i)^2\left(1-\frac{5}{2}e^2\right)\cos[2(M+\omega+\Omega-\theta)] \quad (9)$$

where terms of higher degree in e and $\sin i$ have been discarded. Define the mean motion, n, according to Kepler's third law, $\mu = n^2 a^3$. Since

$$\dot{n} = -\frac{3}{a^2}\frac{\partial R_{22}}{\partial M}, \quad (10)$$

one obtains

$$\dot{n} = +\frac{K^2}{2}\sin[2(M+\omega+\Omega-\theta)], \quad (11)$$

where

$$K = 3n\left(\frac{a_m}{a}\right)(1+\cos i)\left(C_{22}\left(1-\frac{5}{2}e^2\right)\right)^{1/2}. \quad (12)$$

The first derivative of the epoch term for the osculating mean anomaly or mean longitude ($L = M + \omega + \Omega$) involves only the partial derivatives of R_{22} with respect to a, e, and i. The Moon keeps one face oriented toward the Earth so that $L - \theta$ is nearly π. Consequently, the first derivative of the epoch term is proportional to the cosine of a small angle while $\dot{n}$ is proportional to the sine of a small angle. The epoch term contributes primarily to a constant shift in the first derivative of L and only little to its second derivative. We set $\ddot{L} = \ddot{M} = \dot{n}$ and ignore the constant offsets and rapid periodic variations in the mean longitude rate due to the lunar figure, which may be found in Henrard (1980) and Chapront-Touzé (1983). Now we have the relatively simple approximation

$$\ddot{L} = K^2(L - \theta + \pi). \quad (13)$$

Physically, the mean orientation of the Moon is locked onto L so that $L - \theta + \pi$ has only periodic terms. When the angle θ is modeled analytically it is represented as a polynomial in time, plus a sine series. The parameter L represents the mean longitude as it comes from the numerical integration of the equations of motion. If the initial values of L and $\dot{L}$, which are derived from fits of the ranging data, are not precisely compatible with the mean values of θ and $\dot{\theta}$, then there will be a nonperiodic difference which will grow exponentially, since (13) has exponential solutions to its reduced equation. Taking $a/a_m = 221.17$, $i = 6.69°$, $e = 0.055$, $n = 13.368$ rev/Julian yr, and $C_{22} = 22.3\,10^{-6}$ gives $1/K = 588\,\mathrm{yr\,rev^{-1}} = 93.6\,\mathrm{yr\,rad^{-1}}$ or $K^2 = 1''.14\,\mathrm{cy^{-2}}$. An initial misorientation of $1''$ in θ causes an instantaneous acceleration of $1''.14\,\mathrm{cy^{-2}}$, and if the misorientation is a bias rather than a periodic term the acceleration grows monotonically.

There is a simple explanation for the stability of the real physical case. The lunar orientation swings toward alignment with the orbit for orbital longitude variations which are slow compared to the 2.9 yr free libration period in rotation. This response is enough faster than the tendency of the orbit to drift from alignment that there is no instability. In terms of (13), θ adjusts to L faster than L drifts away from θ. It follows that the solution to the problem of the numerical model instability is to numerically integrate a simple physical libration model simultaneously with the orbits, as was done for the ephemeris in this paper.

To explore further the consequences of the instability, we consider θ to be modeled by a quadratic polynomial plus a sine series for the physical libration in longitude τ:

$$\theta = C + \pi + Dt + Et^2 + \tau$$

and include a tidal secular acceleration $\ddot{L}_T$ in the differential equation (13). We first consider the differential equation using the nonperiodic part of θ:

$$\ddot{L}-K^2L=\ddot{L}_T-K^2(C+Dt+Et^2). \tag{14}$$

The solution is

$$L(t)=Ae^{Kt}+Be^{-Kt}+C-(\ddot{L}_T-2E)/K^2+Dt+Et^2, \tag{15}$$

where

$$\begin{aligned} A&=\tfrac{1}{2}\{L(0)-C+(\dot{L}(0)-D)/K+(\ddot{L}_T-2E)/K^2\}\\ B&=\tfrac{1}{2}\{L(0)-C-(\dot{L}(0)-D)/K+(\ddot{L}_T-2E)/K^2\}. \end{aligned} \tag{16}$$

If there is an error in a term of frequency σ and amplitude F in the series for τ, it introduces errors of amplitude $F\sigma K/2(K^2+\sigma^2)$ and $FK^2/2(K^2+\sigma^2)$ in the coefficients A and B. Several useful conclusions can be drawn from the above. The orbit is significantly affected only by the long-period terms (>6 centuries) of physical librations and is insensitive to short-period terms. Any difference between the initial values, rates, and accelerations of the actual orbit and the analytical expression for θ will yield an exponential error in the integrated mean longitude with an exponentiating time scale of 93 yr. Differences of 1″, 1.″07 cy^{-1}, and 1.″14 cy^{-2}, respectively, give similar sized errors.

At the time of our integration, limitations in the lunar theory, especially the long period additive and planetary terms, prevented the modeling of θ with an accuracy better than a few tenths arcsecond. Recent improvements in these long period terms (Standaert, 1980; Chapront-Touzé and Chapront, 1980) as well as the improvements in the main problem by several researchers, have now permitted analytical theories to be fit to numerical integrations over two decades with errors of less than 0.″01 (Chapront and Chapront-Touzé, 1981–1983). It thus becomes practical to again consider modeling θ analytically for integrations of a few centuries as the physical libration calculations become available for these new theories (Eckhardt, 1982). Earlier physical libration calculations are given by Williams et al. (1973), Migus (1980), Eckhardt (1981), and Moons (1981). The long period errors can be expected to increase by an order of magnitude for each two centuries of integration if θ is modeled analytically. For numerical integrations over the decade that lunar laser data are available, modeling is acceptable since the time is short compared to 93 yr and the first two (or three) terms in the expansion of the runoff are compensated by fitting the lunar orbital elements (and secular acceleration).

We relate the above model instability to several comments in the literature. When Oesterwinter and Cohen (1972) used a nonzero S_{22} but did not include the necessary compensating nonzero offset in θ (see Eckhardt, 1972; Kaula and Baxa, 1973; and Williams et al., 1973), they got an anomalous acceleration in longitude. As a consequence they chose a final integration without lunar harmonics. JPL lunar ephemerides prior to LE 37 did not include the physical librations in longitude in the modeling of θ. At that time (1974) the arc of lunar laser data was too short to detect the resulting accelerations. The anomalous acceleration in LE 25 was detected by Van Flandern (1975) by comparing three ephemerides, from different sources, integrated for several decades. Calame and Mulholland (1978b) noticed changes in both the secular acceleration and a periodic term when they added the 14.″3, 271 yr Venus-driven term to the model value of θ in their numerical integration.

The foregoing exposition has concentrated on the errors which can result from injudicious modeling. It is of interest to investigate the analytical solution of the coupled equations for the orbit and physical librations. We write $\theta=L+\pi+\tau$ and $L=L_0+\delta L$, where δL is the perturbed part of the mean longitude. The first approximation to the orbital and librational equations becomes

$$\begin{aligned} \delta\ddot{L}&=K^2(\delta L-\tau)-H\sigma^2e^{i\sigma t}\\ \ddot{\tau}&=3\gamma_L n^2(\delta L-\tau). \end{aligned} \tag{17}$$

The parameter γ_L is a function of the moments of inertia of the Moon, $(B-A)/C$ in conventional notation. The differential equation for δL follows from (13), except that a forcing term has been added which would generate a periodic term $He^{i\sigma t}$ in the orbit in the absence of the coupling through C_{22}. A derivation of the differential equation for τ is given by Eckhardt (1967). A solution can be obtained by subtacting the two differential equations resulting in

$$\begin{aligned} \delta L&=\left(\frac{3\gamma_L n^2-\sigma^2}{3\gamma_L n^2-K^2-\sigma^2}\right)He^{i\sigma t}\\ \tau&=\left(\frac{3\gamma_L n^2}{3\gamma_L n^2-K^2-\sigma^2}\right)He^{i\sigma t} \end{aligned} \tag{18}$$

for the forced terms. The ordinary resonant frequency for physical librations in longitude, $(3\gamma_L)^{1/2}n$ (corresponding to a period of 2.9 yr), is shifted downward by one part in 10^5 to $(3\gamma_L n^2-K^2)^{1/2}$. There is introduced in the orbit an extremely narrow resonance at the same frequency. The amplitudes of some terms in the lunar theory would shift a few centimeters. The solution of the reduced equation is now oscillatory rather than exponential so that the equations of motion are stable during integration.

IV. Numerical representation

The numerical integration program produces a file of positions, velocities, and accelerations at equally spaced times for each component being integrated. Subsequent use of the ephemeris requires an interpolation scheme for recovering any quantity at arbitrary times. Chebyshev polynomials were selected, as they are stable during evaluation and provide an estimate of interpolation error.

The construction and arrangement of the interpolating polynomials is as follows: The entire 4400 yr span is divided into contiguous 64-d intervals. Within each interval the various celestial bodies have their solar system barycentric positions (geocentric position for the Moon) expressed as Chebyshev polynomials, one polynomial representing each Cartesian component. Positions are obtained by polynomial evaluation, velocities by differentiation and evaluation.

Many ephemeris applications require continuity of interpolated position and velocity at the common boundary of adjoining intervals. An algorithm was developed that will accept a set of integrator-supplied positions, velocities, and accelerations of a given component at the end points and at uniformly-spaced interior points of a 64-d interval. The algorithm furnishes the set of coefficients of a Chebyshev polynomial which will provide interpolated position values of the component being represented. This polynomial has the desirable features that (1) when evaluated at any point at which a position value was originally supplied, the polynomial yields the exact original position value; and (2) when once or twice differentiated and evaluated at those same points,

Table 1. Maximum expected position error due to interpolation

Body	Error
Mercury	60 km
Venus	10^{-5}
$E-M$ Barycenter	10^{-4}
Mars	$5\,10^{-4}$
Jupiter	10^{-5}
Saturn	10^{-6}
Uranus	10^{-7}
Neptune	10^{-7}
Pluto	10^{-7}
Moon (geocentric)	$2\,10^{-5}$
Sun	10^{-3}

original velocities and accelerations, respectively, are exactly reproduced. Because the Chebyshev polynomials in adjoining intervals share a common end point during their generation, the interpolated positions and velocities at that end point will be identical (to each other and to the original values supplied by the integrator), regardless of which of the two polynomials is evaluated.

The algorithm makes exhaustive use of the symmetry of Chebyshev polynomials and is comparatively fast, generating about 150,000 coefficients per second on the Univac 1100/81.

This method of producing the coefficients is not a true Chebyshev fit in the minimax sense; however, comparison with actual minimax fits and other interpolation error studies have shown that the polynomials generated by this method comfortably satisfy the most stringent requirements on the ephemeris.

It is important to establish the maximum interpolation error expected when a Chebyshev polynomial is evaluated at arbitrary times. Table 1 shows the comparison of interpolated positions with positions derived directly from the original integration.

The unduly large estimate of Mercury's error is not indicative of a defective integration or of improperly formed Chebyshev coefficients. The 8 d spacing between the input values of position, velocity, and acceleration does not enable the resulting polynomials to provide better agreement with the original integration near Mercury's perihelion. It should be stressed, however, that the representation is exact at the mesh points (times that are an integral multiple of 8 d from JED 2440400.5).

These error estimates are applicable to DE 102 only. Other JPL ephemerides exhibit significantly smaller maximum errors.

V. Adopted constants

The integration requires the numerical values of a number of parameters to be input. Some of these, such as the initial positions and velocities of the planets and Moon, result from the least squares fits and are different in each fit. Other parameters, such as most of the masses and the earth's zonal harmonics, come from outside sources and are only rarely changed. Some parameters, such as the mass of the Earth-Moon system, can be derived from the data, but for convenience are changed only when statistically significant improvements can be made over the standard values.

Table 2 presents the input constants which were not derived from the least-squares fits for DE 102. The masses for Mercury, Venus, and Mars are values obtained from spacecraft tracking during planetary encounters. The mass ratio Sun/(Earth + Moon) is discussed below. For the remaining planets the 1976 IAU values have been retained. The masses for Ceres and Pallas come from Schubart (1974); that for Vesta is from Hertz (1968). For Iris and Bamberga, we have assumed a density equal to that of Ceres (diameter = 1003 km) and diameters of 209 km and 246 km, respectively.

The Earth's radius and zonal harmonics were taken from the SAO Standard Earth 3 model by Gaposchkin (1973, 1974). The radius was adjusted to the newer value of the speed of light used here. At the time of the creation of this ephemeris (1977) the lunar

Table 2. Adopted constants for DE 102

Defining	
Gravitational Constant, k^2 $[=G]$	$(0.01720209895)^2$ au^3 d^{-2}
Speed of light, c	299792.458 km s^{-1}
Mass ratios	
Earth/Moon	81.3007
Sun/Mercury	6023600
Sun/Venus	408523.5
Sun/(Earth + Moon)	328900.53
Sun/Mars	3098710
Sun/Jupiter	1047.355
Sun/Saturn	3498.5
Sun/Uranus	22869
Sun/Neptune	19314
Sun/Pluto	3000000
Asteroid masses $[k^2 m_a]$	
0001 Ceres	$1.746\,10^{-13}$ au^3 d^{-2}
0002 Pallas	$3.847\,10^{-14}$
0004 Vesta	$3.551\,10^{-14}$
0007 Iris	$1.580\,10^{-15}$
0324 Bamberga	$2.576\,10^{-15}$
Terrestrial	
Equatorial radius a_e	6378.156 km
J_2	$1082.637\,10^{-6}$
J_3	$-\ 2.541\,10^{-6}$
J_4	$-\ 1.618\,10^{-6}$
Potential love number k_2	0.29
Lag angle δ	0.04635 rad
Lunar	
Radius a_m	1738.09 km
β_L	$631.26\ 10^{-6}$
γ_L	$227.37\ 10^{-6}$
J_2	$203.822\,10^{-6}$
C_{22}	$22.396\,10^{-6}$
S_{22}	0.0
J_3	$10.44\ 10^{-6}$
C_{31}	$28.6\ 10^{-6}$
S_{31}	$8.8\ 10^{-6}$
C_{32}	$4.82\ 10^{-6}$
S_{32}	$1.71\ 10^{-6}$
C_{33}	$2.7\ 10^{-6}$
S_{33}	$-\ 1.14\ 10^{-6}$

secular acceleration in longitude, $\dot{n}$, was not determined well from the laser data, so we chose the value ($-26''\,\mathrm{cy}^{-2}$) of Morrison and Ward (1975) and derived the value of δ given in the table. Transforming from $\dot{n}$ to the product of the physical parameters k_2 and δ requires a theoretical calculation of the constant of proportionality. Our calculations have been subsequently improved and, based on the expression in Williams et al. (1978), we now estimate the secular acceleration in LE 51 to be $-26''.21 \pm 0''.13\,\mathrm{cy}^{-2}$, the error being in the theoretical constant of proportionality. The calculations of Chapront and Chapront-Touzé (1981, 1982a) would give $-26''.30\,\mathrm{cy}^{-2}$. Other than δ, the same terrestrial constants were used in the LURE 2 lunar ephemeris (Williams, 1977).

The lunar constants in the table are also the same as used in the earlier LURE 2 ephemeris and LLB 5 libration integrations. The values of β_L, γ_L, J_3, C_{32}, S_{32}, and S_{33} came from fits to the lunar laser data made at the time of their generation. The sensitivity of the fits to these six parameters comes predominantly through the physical librations, not the orbit, so we have developed partial derivatives of the range data with respect to these parameters only through the physical librations. In the solutions for the new ephemeris these parameters were adjusted, but during the integrations they were fixed at the LURE 2 values and the simultaneously integrated physical librations were not used to fit data. The remaining third-degree harmonics were taken from averages of values (Williams et al., 1973) derived by several investigators from Lunar Orbiter tracking data. The values of J_2 and C_{22} were derived from β_L, γ_L, and a value of $C/ma^2 = 0.394$ using the constraints in Williams et al. (1973) and Ferrari et al. (1980). The number of digits is for consistency. The values of J_2 and C_{22} in Table 2 are the values also used in the LURE 2 ephemeris. The apparently discordant values in Williams (1977) were from an auxiliary table which was unfortunately edited together with the table of LURE 2 values.

The mass ratio Sun/(Earth+Moon) is the LURE 2 value rounded to two decimal places and was originally derived from analyzing the lunar laser data. The Earth/Moon mass ratio was adopted in the LURE 2 set as a weighted average of spacecraft results from Null (1970), Jordan et al. (1972), and Wong and Reinbold (1973).

Since the adoption of the constants given in this section, many improvements have been made. For slightly improved earth harmonics we refer the reader to the 1979 IUGG set. For lunar constants and mass ratios the results of Ferrari et al. (1980), Cappallo (1980), and Dickey et al. (1982) are recommended. Lunar laser data now yield a good determination of the lunar secular acceleration (Calame and Mulholland, 1978; Williams et al., 1978; Dickey et al., 1982; and Dickey and Williams, 1982), the last reference giving $\dot{n} = -25''.1 \pm 1''.3\,\mathrm{cy}^{-2}$.

For the lunar orbit, the quantity most sensitive compared to its uncertainty and dependent on Table 2 is the secular acceleration. Orbit accuracies will be discussed in VII.D, VIII.B, and IX.

VI. Observational data

A. Lunar laser range data

The lunar laser range (LLR) data consist of time-of-flight measurements from McDonald observatory to any one of four retroreflectors on the Moon and back again. The retroreflectors are at the Apollo 11, 14, and 15 landing sites and on the Lunakhod 2 vehicle. These 2085 range points are distributed from August 1969 to January 1977. The normal points through 1973 have been published by Abbot et al. (1973), Shelus et al. (1975), and Mulholland et al. (1975). The LLR data are deposited in the National Space Science Data Center. During the least squares fit the ranges have been weighted according to the instrumental errors which accompany each point. The general trend is toward improving accuracy with time. The simple post-fit rms residual is 2.78 ns, equivalent to 42 cm in one-way range.

B. Planetary data

There were 48,479 observations used in the planetary solution for DE 102. These come from six major sources which are described below. For the solution, each observational equation was normalized by multiplying it by the factor, $1/\sigma_0$, where σ_0 is the *a priori* standard deviation of one observation. From previous experience, we were able to assign values to these σ_0 which were approximately equal to their post-fit rms residuals.

In actuality, the rms residuals quoted in Tables 3a–c were taken from the fits for DE 96 (Standish et al., 1976). The corresponding values for DE 102 differ by less than 1%.

1. Optical

The optical observations come from the Six- and Nine-Inch Transit Circles of the U.S. Naval Observatory (USNO). They cover the time span 1911–1971 and have been discussed by Oesterwinter and Cohen (1972) and by O'Handley et al. (1969).

All of the optical observations have been reduced to the FK 4 Catalogue system using the tables given in the Second Series of the *Publications of the U.S. Naval Observatory*, Vol. XIX, Part II.

Three types of systematic trends have been noticed in the optical residuals with previous ephemerides. These trends were removed empirically in the solution for DE 102 and are given here.

a) The optical data covering the years 1962–1971 have not had day corrections applied for the Sun, Mercury, and Venus (the three bodies observed during daylight). Consequently the corrections applied in DE 102 use coefficients determined in the solution itself. The forms of the correction are

$$\Delta\alpha = A_1 + A_2 \sin\delta + A_3 \cos h_\odot$$

$$\Delta\delta = D_1 + D_2 \sin\delta + D_3 \cos h_\odot,$$

where δ is the declination and $h_\odot$ is the hour angle of the Sun (i.e., time of day). The corrections $\Delta\alpha$ and $\Delta\delta$ are to be subtracted from the observed values of α and δ.

b) Secular-like drifts, due among other things to an inaccurate value of precession and an equinox motion in the FK 4, have been removed using the corrections

$$\Delta\alpha = (\Delta k + \Delta n \sin\alpha \tan\delta) T_{50}$$

$$\Delta\delta = \Delta n \cos\alpha T_{50},$$

where T_{50} is the time in centuries since 1950. The factors Δk and Δn are applied to all optical observations of the planets and Sun, and they are determined empirically in the solution. If one assumes that these parameters come from precession error and equinox drift exclusively, the following relations apply:

$$\Delta k = -\dot{E} + \Delta p \cos\varepsilon,$$

and

$$\Delta n = \Delta p \sin\varepsilon$$

where $\dot{E}$ is the equinox drift, Δp is the correction to precession, and ε is the value of the earth's obliquity. The corrections $\Delta\alpha$ and $\Delta\delta$ are subtracted from the observed values of α and δ.

c) A systematic trend, called the "Phase Effect", is noticeable when the residuals are displayed with respect to time near planetary opposition (or superior conjunction for Mercury and Venus). They evidently arise from observational difficulties in relating the measured portion of the partially illuminated disk to the center of mass of the planet.

There are three types of measurements of a planetary disk: *(i)* the center of light of the complete object, used usually for Mercury, sometimes for Venus and always for Uranus, Neptune and stars; *(ii)* the illuminated edge only, in right ascension and declination, used sometimes for Mercury and usually for Venus; and *(iii)* both the illuminated edge and the terminator, each in right ascension and declination, used always for Mars, Jupiter and Saturn. The USNO has applied corrections for each of these three types of observations; those for type *(i)* are empirical while those for types *(ii)* and *(iii)* are rigorously derived from geometric considerations. These formulae are given in Appendix II, Volume IV of the USNO publications.

For DE 102, the empirical corrections were *removed* from the observations of type *(i)*, while the corrections for types *(ii)* and *(iii)* were retained. In addition, the following three corrections were respectively applied to the three types of observations, with the coefficients being determined in the solution for DE 102:

$$(i)\quad \begin{Bmatrix}\Delta\alpha\\ \Delta\delta\end{Bmatrix} = \frac{s}{\varrho}\begin{Bmatrix}\sin\Theta\\ \cos\Theta\end{Bmatrix}[C_0 + C_1 I + C_2 I^2 + C_3 I^3]$$

$$(ii)\quad \begin{Bmatrix}\Delta\alpha\\ \Delta\delta\end{Bmatrix} = \begin{Bmatrix}\sin\Theta\\ \cos\Theta\end{Bmatrix}[L_0 + L_1 I + L_2 I^2 + L_3 I^3]$$

$$(iii)\quad \begin{Bmatrix}\Delta\alpha\\ \Delta\delta\end{Bmatrix} = \begin{Bmatrix}\sin\Theta\\ \cos\Theta\end{Bmatrix} B_k \sin 2i,$$

where $k=4,\ldots,8$ for Mars, ..., Neptune, s is the planet's semi-diameter at unit distance, ϱ is the planet's geocentric distance, i is the phase angle (Earth-Sun separation angle subtended at the planet), Θ is the position angle of the midpoint of the illuminated edge of the planet's visible disk (measured eastwards from north), and where $I=i/90°$. The forms of these formulas were chosen arbitrarily to fit the observed residuals. For Uranus and Neptune, formula *(iii)* was used even though their measurements were of type *(i)*. In any case, the phase effect for these two planets is negligible.

The *a priori* standard deviations in right ascension and declination were taken as $1''.0 \sec\delta$ and $1''.0$, respectively, for the Sun, Mercury, and Venus, and $0''.5 \sec\delta$ and $0''.5$, respectively, for Mars through Neptune.

The number of observations for each body and the rms post-fit residuals about the mean for the optical data are shown in Table 3a.

Table 3a. Optical observations

Planet	α		δ		Totals
	N	σ_{rms}	N	σ_{rms}	
Sun	8223	0".81	7930	0".83	16153
Mercury	2412	0.98	2339	0.85	4751
Venus	3566	1.17	3386	0.89	6952
Mars	830	0.63	804	0.55	1634
Jupiter	1068	0.50	1030	0.51	2098
Saturn	1091	0.53	1040	0.54	2131
Uranus	1048	0.37	1034	0.45	2082
Neptune	1037	0.40	1015	0.50	2052
Totals	19275		18578		37853

Table 3b. Radar observations

Source	Mercury		Venus		Mars		Totals
	N	σ [μs]	N	σ [μs]	N	σ [μs]	
Arecibo	106	17.1	248	8.1	30	83.3[a]	384
Haystack	217	10.0	219	9.2	2745	12.8	3181
Millstone			101	94.8[a]			101
Goldstone 13			294	38.2[a]	4	10.0	298
Goldstone 13/14	9	9.2	14	7.6	300	11.4	323
Goldstone 14	22	8.6	44	13.4	699	10.7	765
	354		920		3778		5052

[a] These data are mostly pre-1967 and are therefore of lower quality than later data. They were severely down-weighted in the solution for DE 102

Table 3c. Mariner 9 range points

N	Julian date	σ [μs]
77	2441272–2441361	0.25
81	2441389–2441540	0.29
487	2441541–2441555	0.78
	2441577–2441602	
158	2441556–2441575	2.50
803		

2. Radar

Radar time-delay measurements from Mercury, Venus, and Mars have come from six sources: Arecibo Ionospheric Observatory, Haystack (MIT), Millstone Hill (MIT), Goldstone Deep Space Station (DSS) 13 (JPL), Goldstone DSS 13/DSS 14 Bistatic (JPL), and Goldstone DSS 14 (JPL). The *a priori* standard deviation assigned to these data varied according to source, planet, and year. The number of radar data points for each planet and their post-fit rms residuals are shown in Table 3b. One microsecond of time delay is equivalent to 150 m of one-way range.

Occultation measurements of the Martian surface by Mariner 9 have shown that the shape of the surface can be approximated by a triaxial ellipsoid. This determination and its implications for radar ranging have been discussed by Standish (1973). The radar time delays from Mars have been computed using this triaxial model. The whole ellipsoid is scaled according to the mean equatorial radius of the planet, the only figure-related parameter estimated in the solution for DE 102. The shape and orientation of the ellipsoid are unaltered.

The surfaces of Mercury and Venus are approximated by spheres.

3. Mariner 9 range points

The Mariner 9 Navigation Team combined 803 range points to the Mars Orbiter with positions of the orbiter relative to the center of mass of Mars in order to produce accurate Earth-Mars ranges from November 1971 to October 1972. These data, summarized in Table 3c, exist in four sets according to their proximity to the Martian solar conjunction (JD 2441568), when the 2200-MHz ranging signal passed within 4 solar radii of the sun at heliographic latitude +79°. The uncertainties in the propagation of the signal through the corona are reflected by the post-fit rms residuals.

Besides the standard relativistic time delay in the radar signals between the Earth and a planet (Shapiro, 1964), there is a delay caused by the electron density in the solar corona. This has been discussed by Muhleman et al. (1977). The following formula for corona delay $\Delta\tau$ (μs) was used in processing the radar and Mariner 9 data in DE 102:

$$\Delta\tau = \frac{40.3}{cf^2}\int_{P_1}^{P_2} N_e\, ds,$$

where c is the speed of light (cm s^{-1}), f is the frequency (MHz) of the radio carrier signal, N_e is the electron density (cm^{-3}), and the integration is carried out over the linear distance (cm) from point P_1 to point P_2 in space. The electron density was assumed to have the following form:

$$N_e = \frac{A}{r^6} + \frac{B}{r^{2+\varepsilon}}$$

with the solar distance r expressed in units of the solar radius.

The values of the constants used for DE 102 are

$A = 1.3\,10^8$ cm^{-3}

$B = 0.5\,10^6$ cm^{-3}

$\varepsilon = 0.0$.

These values are consistent with the corona derived from Mariner 6 and 7 data by Muhleman et al.

4. Pioneer 10 and 11

The Pioneer Navigation Teams at JPL provided Earth-Jupiter ranges by combining Earth-spacecraft ranges with positions of the spacecraft relative to Jupiter's center of mass at the times of encounter (JD 2442020 and JD 2442385). The *a priori* standard deviations were 50 μs for each.

5. Mars radar closure

There were 306 "closure points" from the Mars radar data taken during the oppositions of Mars in 1971, 1973, and 1975. These closure points are pairs of days, each spanning at least two years, during which the observed points on the surface of Mars are nearly identical with respect to Martian longitude and latitude. Since the same topographical features are observed during each day, the uncertainty introduced by the topography of Mars may be eliminated by subtracting the residuals of one day from those of the other day. The remaining difference is then due only to the ephemeris drift between the two days. These points had *a priori* standard deviations of about 1 μs.

6. Viking orbiter range points

The Viking Navigation Team at JPL provided Earth-Mars range measurements by combining Earth-spacecraft ranges with positions of the spacecraft relative to the center of mass of Mars. These data encompass 242 d, commencing on June 20, 1976 (JD 2442949.6–2443191.0). Since the measurements were taken at two frequencies, the Navigation Team was able to calibrate the effect of the solar corona electron content and thereby remove its effect on the data. As such, no modeling of the corona was necessary for using these data in the solution for DE 102.

There were 2498 points from Orbiter I and 1965 points from Orbiter II. The *a priori* standard deviation of these data were computed from

$$\sigma = [0.0038 + 0.0062\, e^{(5.28 - 0.033D)}]^{1/2}\ \mu\text{s},$$

where D is the number of days on either side of Mars' solar conjunction (JD 2443108). For $D > 160$, $\sigma = 0.1$ s was used.

VII. Data fits

In discussing the creation of DE 102/LE 51 it is stressed that though there were separate least squares fits to the planetary and lunar data, the integration of the lunar and planetary orbits was done simultaneously. First, the planetary data were fit; then the resulting new planetary starting conditions were integrated with old lunar starting conditions to produce a preliminary ephemeris (DE 101). Then, the planetary initial conditions were held fixed and several iterations of lunar fits and joint integrations were performed until the orbit had converged. As a part of one of the intermediate iterations, a simultaneous rotation of the lunar and planetary orbits was carried out to bring the earth's equator into consistent alignment with the ephemerides. This rotation will be described later (VII.C).

A. Planetary least squares solution

There were 71 parameters in the full rank solution for the planets in DE 102. 46 of these parameters were used to adjust the initial conditions of the planets Mercury through Neptune. Those for Pluto were taken from DE 69 (O'Handley et al., 1969). In addition, the plane of the Earth-Moon barycenter's heliocentric orbit was left unchanged from DE 96 (Standish et al., 1976) by not solving for its two defining parameters. Subsequently, after the solution, the entire set of planetary initial conditions was rotated into alignment with the lunar solution, as mentioned above.

As described before (VI.B.1b), the parameters Δk and Δn are introduced into the solution in order to account for observed secular-like drifts in the optical data. They arise mainly from the fact that the mean motions of the inner planets, being determined primarily from the strength of the ranging data, are not consistent with those implied by the optical observations. It is tempting to attribute the resulting values solely to a precession correction Δp and to an equinox motion $\dot{E}$, especially since the solution values of $0''.726\,\text{cy}^{-1}$ and $1''.426\,\text{cy}^{-1}$ are reasonably close to those (Fricke, 1968, 1982) of $1''.100\,\text{cy}^{-1}$ and $1''.275\,\text{cy}^{-1}$, respectively. However, it must be realized that the optical observations could very well be subject to further systematic errors, such as catalogue offsets and seasonal errors, which would also influence the derived values of Δk and Δn.

The list of values resulting from the planetary least squares solution is given in Table 4.

Table 4. Parameters from the planetary data fits for DE 102

Orbital parameters
(Corrections for all planets except Pluto; Earth-Moon barycenter orbital plane held fixed at epoch)

Scale factor

AU	149597870.684 km au^{-1}

Optical drift parameters

Δk	$-0''.760$ cy^{-1}
Δn	$+0''.289$ cy^{-1}
implying	
$\Delta p =$	$+0''.726$ cy^{-1}
$\dot{E} =$	$1''.426$ cy^{-1}

Optical day/night corrections

A_1	$-0''.12$	D_1	$-0''.36$
A_2	$+0.20$	D_2	-1.38
A_3	$+0.18$	D_3	$+0.50$

Optical phase corrections

C_0	-0.03	L_0	$-0''.13$	B_4	$0''.42$
C_1	$+0.45$	L_1	2.69	B_5	0.98
C_2	$+0.39$	L_2	-2.25	B_6	0.84
C_3	-0.24	L_3	0.65	B_7	0.39
				B_8	1.21

Planetary radii (from radar ranges)

Mercury	2439.958 km
Venus	6051.813
Mars	3396.644[a]

[a] Mean equatorial radius of triaxial ellipsoid

Table 5. McDonald observatory coordinates used in DE 102 (cylindrical coordinates)

Spin radius r_s	$= 5{,}492{,}414.39 \pm 0.28$ m
East longitude λ	$= 255°.9781805 \pm 0°.0000067$
Equator height z	$= 3{,}235{,}697.45 \pm 0.48$ m

B. Lunar least squares solution

After choosing the constants an initial integration of the Moon and planets was performed. Between the initial and final integrations were several cycles of fits and integrations which served to fit the lunar orbit to the laser data and to rotate the whole lunar and planetary system about three orthogonal axes. The weighted least squares fits to the lunar ranges had 39 parameters: 6 lunar orbital elements, 2 parameters to orient the equator of the earth with respect to the ecliptic, 6 initial conditions for the lunar physical librations (3 angles and 3 angular rates), 6 parameters of the lunar gravity field (β_L, γ_L, C_{30}, C_{32}, S_{32}, S_{33}), 12 selenocentric coordinates for the four retroreflectors, 3 geocentric coordinates for McDonald Observatory, and 4 parameters modeling UT 1 (a rate, a pair of annual terms, and a long-period term). This choice of parameters is a conservative set; solving for 6 additional parameters [the three remaining third degree lunar harmonics, the secular acceleration of the Moon, the Nordtvedt term, and the gravitational constant times the mass (Gm) of the Earth-Moon system] reduced the rms residual by 0.12 ns (2 cm). The first four of the additional parameters were considered too uncertain in the solution to provide a significant improvement; the Nordtvedt term was set to zero since it represents a violation of the equivalence principle of general relativity which has not been observed (Williams et al., 1976; Shapiro et al., 1976); and Gm of the Earth-Moon system was left unchanged, since its small change would also have required a change in the planetary starting conditions. These 45-parameter solutions were performed to provide comparisons, but the smaller set of parameters was felt to be more compatible with our primary objective of generating a new ephemeris. The final 39-parameter solution using LE 51 gave a 2.78 ns rms residual (42 cm) and a 45-parameter solution gave 2.66 ns (40 cm). The coordinates of the intersection of axes of the McDonald Observatory 2.7 m telescope are taken from the former solution and presented in Table 5. The derived longitude depends on the equinox offset of the ephemeris (Williams and Melbourne, 1982) and is consequently shifted from other published values by the $0''.67$ rotation of Sect. VIII.A.1. A more recent solution for masses, lunar gravity field, and observatory and retroreflector coordinates is presented and discussed by Ferrari et al. (1980).

C. Combined orientation

As part of the iterations of the lunar fits and integrations, a rotation was applied to the planetary starting conditions which had been generated by fitting the planetary data alone. Range data to the planets are sensitive to the relative orientations of the planets, but the absolute orientation in the planetary fits is controlled solely by the optical data. The few-decimeter fits of the lunar range data contain a surprising amount of orientation information. Projected onto the surface of the Earth, 1 arc s in orientation is 31 m in displacement. Though this sensitivity is reduced when projected into the lunar direction, the range data implicitly contain orientation information of order $0''.01$. Since the ranging station sits on a spinning Earth, the true terrestrial equator of data can be sensed as a reference plane. The orbit plane of the Moon effectively precesses about the ecliptic in 18.6 yr, implying that the lunar range data contain information on the orientation of both the lunar orbit and the Earth's heliocentric orbit with respect to the equator. The fact that the lunar data cover less than half of the precession time means that there is incomplete separation of the orientations during the solution. The expression for the radial distance to the Moon also contains solar perturbation terms sensitive to the alignment of the lunar node and inclination with respect to the ecliptic. (Note that the orientations of the ecliptic and lunar orbit are determined with respect to the true equator of date.) The relation with the equator of B 1950.0 depends upon the adopted time-varying model for the precession, obliquity, and nutation from the weighted mean time of our observations (about 1974) to B 1950.0. The lunar data analysis used the conventional (pre-IAU 1976) expressions for the general precession and obliquity change. If the new (1976 IAU) expressions (Lieske et al., 1977; Lieske, 1979) are to be used the ephemeris should be adjusted to preserve the orientations at 1974. We believe that at present the relative orientations of the three planes are determined to an uncertainty of about $0''.015$.

The lunar range fits include parameters (θ_x and θ_y) for right-handed rotations of the earth about two axes at $\alpha = 0°$, $\delta = 0°$, and $\alpha = 90°$, $\delta = 0°$ while holding the planetary ephemeris, and hence the ecliptic, fixed. The solution values of $\theta_x = -0''.084$ and $\theta_y = +0''.177$ with respect to the initial planetary ephemeris were applied as rotations of opposite sign to the whole system of lunar

Table 6a. Heliocentric planet states, geocentric Moon state, and solar system barycentric Sun state at selected epochs. The units are au and au d^{-1}

	x	y	z	$\dot{x}$	$\dot{y}$	$\dot{z}$
JD = 2440000.50	1968 MAY 24 00:00:00					
MERCRY	-.356131898316646	-.079923616931072	-.002105034672280	-.000650606969612	-.023344965640621	-.012435101883681
VENUS	.513143484551837	.475694506541018	.181951575578733	-.014303994571041	.012689940711713	.006621793762169
EMBARY	-.465602695066752	-.825201166429926	-.357836102451260	.014997038811555	-.007311441230445	-.003170601480761
MARS	.379616473387926	1.357046616627028	.612718066677804	-.013009572479121	.004090125563618	.002226646439465
JUPITR	-5.003201204907751	1.826864769523277	.906019138038051	-.002930176019319	-.006130655617238	-.002558438769334
SATURN	8.967421164152340	2.645579909524743	.706191309448817	-.001919249880525	.004893473966354	.002106222174576
URANUS	-18.279812801846174	.551243739765469	.499839838126083	-.000186069616241	-.003773324031039	-.001650648835062
NEPTUN	-17.415827756069245	-23.128533031031773	-9.036208583689424	.002547542835049	-.001632113173717	-.000732800107223
PLUTO	-30.542074977396260	.728360972156998	9.485336035964553	.000166968206885	-.003151291523364	-.001047414721253
MOON	.002415066854972	.001096922837270	.000516582280778	-.000240377381614	.000443996805375	.000247146429290
SUN	.003919321270926	-.001324616245090	-.000622788929937	.000003211870019	.000004692709701	.000001943365000
JD = 2440400.50	1969 JUN 28 00:00:00					
MERCRY	.355792583292400	-.095534548515480	-.087713219145494	.003708702223901	.024849789709197	.012926880605116
VENUS	.663351526104238	-.355904487317372	-.198487669529248	.011156875320646	.015488930738822	.006275166193051
EMBARY	.103696319474665	-.927833598248090	-.402340007890888	.016833529266915	.001555077255782	.000674240852369
MARS	-.132473821913757	-1.326985054158883	-.605554764685246	.014482202982455	.000075394335056	-.000354111057258
JUPITR	-5.394193291553878	-.771008120047268	-.198915059073805	.001005654748533	-.006535020682084	-.002828109099922
SATURN	7.948243636719564	4.507187023227101	1.519958994654949	-.003159200139015	.004366270522430	.001941907786670
URANUS	-18.282750855798804	-.958434031884277	-.161586773687624	.000171380264953	-.003769850775359	-.001654199462772
NEPTUN	-16.371633528829260	-23.761703783929610	-9.321653368565120	.002622812028382	-.001532924450898	-.000694062397851
PLUTO	-30.452355966380919	-.532549613697370	9.059463360111604	.000282060048511	-.003152131875254	-.001081645825637
MOON	-.000835696144214	-.001985441942846	-.001083269200246	.000598752743373	-.000174151775434	-.000088476864467
SUN	.004527775417440	.000723365869243	.000243736732666	-.000000283960641	.000005183018054	.000002231362297
JD = 2440800.50	1970 AUG 02 00:00:00					
MERCRY	-.347281920716391	-.253820790418240	-.100252977982116	.011643568001284	-.017968873793638	-.010819114061169
VENUS	-.272923962286769	-.619188066470830	-.261789347211002	.018600749299038	-.006590455348420	-.004144650979231
EMBARY	.638824863056050	-.723464449022686	-.313719906075961	.013086989741705	.009880617382417	.004284477300128
MARS	-1.043278049088229	1.149606436844376	.555691494879293	-.010285734779613	-.007076402922278	-.002972130224440
JUPITR	-4.241128326947548	-3.149119618291833	-1.247309466117799	.004626328984462	-.005059611156843	-.002283652292940
SATURN	6.459592864736689	6.101147983100087	2.243389283768249	-.004252245269350	.003559252961775	.001655564203679
URANUS	-18.143115258806633	-2.460584248417711	-.821739877441121	.000526204163907	-.003735779666599	-.001644318363017
NEPTUN	-15.308270983774163	-24.354331906136272	-9.591216965150027	.002693305697018	-.001429470425948	-.000653427179519
PLUTO	-30.316286814236456	-1.792529991905536	8.620226640260410	.000398622952872	-.003146652697593	-.001114236167781
MOON	-.001601309026202	.001957203235842	.000968482143504	-.000458407901440	-.000278698567938	-.000170697508693
SUN	.003793062435931	.002631816324760	.001079306784696	-.000003443608740	.000004037830291	.000001810724573

Table 6b. Libration Euler-angle states at selected epochs, in rad and rad d^{-1}

JD = 2440000.5 1968 May 24 0:00:00

$\phi = -2.02126089300823206\ 10^{-2}$ $\quad \dot{\phi} = -4.72630701310065239\ 10^{-5}$
$\theta = 3.83103602337437716\ 10^{-1}$ $\quad \dot{\theta} = 4.20077869488481184\ 10^{-6}$
$\psi = 2.42325263496018642\ 10^{-2}$ $\quad \dot{\psi} = 5.61707911515954610\ 10^{-5}$

JD = 2440400.5 1969 Jun 28 0:00:00

$\phi = 5.93464084784960331\ 10^{-3}$ $\quad \dot{\phi} = 1.05662466745666694\ 10^{-4}$
$\theta = 3.82409065087238434\ 10^{-1}$ $\quad \dot{\theta} = 2.30262134992888838\ 10^{-5}$
$\psi = 0.0$ $\quad \dot{\psi} = -1.24093888386235919\ 10^{-4}$

JD = 2440800.5 1970 Aug 2 0:00:00

$\phi = 3.27032335106893298\ 10^{-2}$ $\quad \dot{\phi} = 9.90208595640356422\ 10^{-5}$
$\theta = 3.85226644196030775\ 10^{-1}$ $\quad \dot{\theta} = -7.23251966664739728\ 10^{-5}$
$\psi = -2.51161735346522412\ 10^{-2}$ $\quad \dot{\psi} = -7.88484391951160019\ 10^{-5}$

and planetary starting conditions for the next integration while holding the equator fixed. As an attempt to achieve a dynamical equinox, a rotation of $+0''.683$ was applied to the right ascensions. This latter number was the equinox offset determined by Van Flandern (1977, private communication) for DE 97/LE 47. This latter rotation failed to achieve a dynamical equinox by $0''.1$ because the addition of new planetary data, after the generation of DE 97, caused changes in the planetary orbits which, when coupled with the lunar derived rotations, resulted in the offset.

Table 6a lists the positions and velocities of the planets, Moon, and Sun at the epoch of solution, JED 2440400.5, and at the neighboring epochs 2440000.5 and 2440800.5. The solar system states at these adjoining epochs may prove useful for comparison with other integrations. The states of the nine planets are heliocentric; the lunar state is geocentric; and the solar state is with respect to the solar system barycenter. The units are au and au d^{-1}.

The libration states at the same three epochs are given in Table 6b. From the nature of its definition the angle ψ (denoting the angular displacement of the selenographic meridian from the earth's equator) grows rapidly with time, changing by 2π radians per lunar revolution. To limit the magnitude of the numbers

carried by the numerical integrator, a linear polynomial was removed from the initial conditions for ψ presented to the integrator. In all calculations the actual values of ψ and $\dot{\psi}$ used are:

$$\psi(t) = \psi_{\text{int}}(t) + \psi_0 + \psi_1 t$$

$$\dot{\psi}(t) = \dot{\psi}_{\text{int}}(t) + \psi_1$$

where $\psi_{\text{int}}(t)$, $\dot{\psi}_{\text{int}}$ denote the angle and rate provided by the integrator;

$\psi_0 = 1.28196362980467391$ rad ;

$\psi_1 = 0.229970890283347893$ rad d^{-1} ;

t is the time in days from the epoch of initial conditions.

D. Orbit accuracies

The discussion of accuracies is given in three parts, according to the dominant data type used: the four inner planets have very good relative orbits, due largely to the ranging data; the orbits of the more distant planets depend on optical data and are less accurate; and the lunar orbit is well determined by the laser ranging data. In all cases the accuracy of the ephemerides will degrade as one extrapolates outside the span of observed data. It is convenient to describe the accuracy of the ephemeris in terms of the orbital elements implicit in the initial positions and velocities of the integration. Osculating elements can be easily derived from initial conditions, but the recovery of mean elements requires comparisons with theories (see the Introduction for references). This section interprets the accuracies and relations between the range-dominated orbital parameters. Much of this interpretation is known in the analysis community but has not been published.

For the four inner planets the range data dominate the accuracy of the semimajor axes, eccentricities, mean anomalies, and mean motions, as these parameters enter directly into distance calculations. Well determined in a relative sense are the ecliptic mean longitudes, perihelion directions, and the orientations of the orbit planes. The system of the four inner planets can be rotated as a unit by three constant arbitrary angles (though not by arbitrary angular rates) without changing the relative distances. Some combination of other data types and adopted conventions sets the absolute orientation of the system. It is a result of the geometry of planetary ranging that the difference between the mean heliocentric longitude of a planet and that of the Earth is well determined and, after a span of time, so are the relative mean motions. At a distance of one astronomical unit, 725 km subtends an angle of 1″, so that the kilometer-sized radar ranging accuracies previously given imply accuracies (1) for the relative longitudes of a few marcs and (2) for the relative mean motions of a marcs yr^{-1} or less. Relative longitudes for Venus, Earth and Mars show realistic accuracies of 0.″003 or less at the 1969 epoch; that for Mercury, somewhat larger. A contribution to the error arises from the displacement of the epoch from the center of the data spans.

Since the orbits of the planets are elliptical, there are periodic displacements from circular motion of amplitude ae in the radius and $2ae$ in the longitude direction, where a is the semimajor axis and e is the eccentricity. These displacements will have measurable projections into the range direction so that both the amplitude and phase can be determined. The uncertainties in ae are less than 1 km for Mercury and Venus, and less than 100 m for Earth and Mars, the latter pair being better determined by the ranges to spacecraft orbiting Mars. As the phase of these terms gives the mean anomaly, the accuracy of the mean anomaly should scale directly as the accuracy of the range data and inversely as the product ae. Of the four planets Mars has the most accurately determined mean anomaly. In order of increasing mean anomaly uncertainty the earth, Mercury, and Venus follow. Given the mean anomaly [the difference between the mean longitude and the perihelion longitude ($\ell_j = L_j - \tilde{\omega}_j$)], and the differential mean longitudes $L_j - L_k$ it follows that the differences between all sixteen combinations of mean longitudes and longitudes of perihelia $L_k - \tilde{\omega}_j$ and the six combinations of perihelia $\tilde{\omega}_j - \tilde{\omega}_k$ are known. Since the mean anomaly error is proportional to $1/e$, while the differential longitudes are better determined, the accuracies of the last two differences above are limited by the mean anomaly errors; hence the differences with Mars' perihelion are the most accurate and those with Venus' perihelion the least accurate.

Since ranges give mean anomalies, the mean anomaly rates will result after a span of time. A system of four inertial (sidereal) mean motions is yielded by the combination of (1) the precise differential mean motions, (2) the most accurate of the individual planetary mean anomaly rates, and (3) the expectation that the perihelion precession rates are given well by the modeling of accelerations in the integrator. Mars has the most accurate mean anomaly rate so that the connection of the four inner planets to an inertial system rests on the Mariner 9 and Viking orbiter range data. During the time spanned by these blocks of data the observational noise on the mean motions of the earth and Mars is about 0.″01 cy^{-1}. The error in the longitude of perihelion rate for Mars, about 0.″013 cy^{-1}, is dominated by the errors in the masses of the Jovian planets. Because of the two short spans of spacecraft data, errors which cause short-period signatures will also corrupt the mean motion. Thus the error of Jupiter's mass contributes 0.″03 cy^{-1} to the mean motion error. For longer time scales the limiting error (about 0.″025 cy^{-1}) for inertial mean motions results from long period terms in the Martian longitude induced by asteroids of uncertain mass (Williams, 1984). Thus the resulting error in the long-time, inertial mean motions for the earth and Mars is about 0.″04 cy^{-1}. For Venus this uncertainty is about 0.″06 cy^{-1} and for Mercury about 0.″14 cy^{-1}.

The product of the gravitational constant and the solar mass is a fundamental constant of the solar system and is defined in units of au^3 d^{-2} (Table 2). With accurate mean motions it follows from Kepler's third law that the planetary semimajor axes will be well determined in astronomical units. The "range" measurements are really roundtrip light times, but since the speed of light is a second fundamental constant these are equivalent to measurements in kilometers. The geometry of ranging also gives information on the semimajor axes in kilometers, and the ratio to the values in astronomical units gives the value of the astronomical unit in kilometers, [equivalent to determining Gm_{Sun} in laboratory units (km^3 s^{-2})]. The spacecraft ranging data to Mars again dominate the accuracy of this scaling factor; the less accurate radar data adjusts the planetary radii. At the time that the Viking orbiter range data were first added to the older data, the determinations of the mean motions of the inner four planets decreased 0.″5 cy^{-1}, the au shrank by 700 m, and the planetary radii shrank by several hundred meters. More than an order of magnitude improvement in the accuracy of the mean motions and the au (now ±30 m) was made in a single step.

The relative orientations of the orbit planes of the inner four planets are less well determined than many of the above orbital

parameters because they enter the ranging equations at second degree, but they still improve upon determinations based on optical data alone by an order of magnitude. The estimated errors with respect to the ecliptic are a few hundredths of an arcsecond for Mercury, a hundreth arcsecond or less for Venus, and a few marcs for Mars. As previously described (Sect. VII.C) these orbit planes were collectively oriented with respect to the earth's equator and the lunar orbit plane during the fits to the lunar laser data. It is estimated that this orientation is accurate to 0".015 at 1974, with corrections for the precession constant needed at other times as described.

For the Moon the mean orbital elements which affect its geocentric distance will be strongly determined by the laser ranging data. The eccentricity is implicitly determined to a few parts in 10^9 and the mean anomaly to a few marcs. There is a strong determination of the differential geocentric lunar and solar ecliptic longitudes resulting from strong solar perturbations on the lunar distance (amplitudes of about 3000 km and 4000 km for the two leading terms). During the span of the observations the differential longitudes are known to about 0".005. Outside the data span the error in the lunar longitude is dominated by the uncertainty in the lunar tidal acceleration. Since the generation of LE 51, better values of the secular acceleration have been determined. The most recent value of $-25''.1 \pm 1''.3\,\mathrm{cy}^{-2}$ (Dickey and Williams, 1982) would indicate that in LE 51 a correction of $0''.55 \pm 0''.65\,\mathrm{cy}^{-2}$ is needed to the lunar longitude. For historical observations the accuracy of the ecliptic longitude of the Moon is still inferior to that of the four inner planets. The mean distance of the Moon is set by the adopted value of the Sun/(Earth + Moon) mass ratio in Table 2. Improved values (Dickey et al., 1981) indicate that a correction of -8 ± 6 m is needed. The large uncertainty compared to the decimeter laser data itself results since one of the selenocentric reflector coordinates is nearly parallel to the Earth-Moon vector, and hence separates from it only weakly.

VIII. Adjustments to DE 102

As mentioned in the previous section, the orientation of the reference frame of DE 102 does not coincide with any of the standard reference systems commonly used in astronomy, such as the FK 4 at 1950 or the dynamical equinox of 1950 or of 2000. Furthermore, since the creation of DE 102, there have been a number of improvements incorporated into the more recent ephemerides produced at JPL. These improvements have been the result of newer and more extensive sets of observational data as well as more refined data reductions. Such improvements have led to revised values of some of the constants used in the integrations as well as adjustments to the lunar and planetary orbital initial conditions. However, none of the newer ephemerides has been integrated more than two centuries in time and so it is not possible to replace DE 102 with a newer ephemeris for use at times which are very far from the present epoch. It is possible, however, to directly modify DE 102 so that it closely approximates what a newer ephemeris would give if it were to be integrated over the time span of DE 102. This is possible, especially, since the equations of motion described in Sect. II have remained unchanged for ephemerides created since DE 102.

This section discusses how one may re-orient the reference frame and/or improve the positions and velocities of DE 102 in order to better approximate those of the more recent JPL ephemerides. It was, however, the analysis of the obliquity and equinox offset from the long span of DE 102 which permitted these parameters to be determined for the shorter, more recent ephemerides.

A. *Re-orientation of axes*

The simplest change to DE 102 is a constant rotation applied to the positions and velocities at each time. The rotation may be expressed in the form of a 3×3 matrix, the result of successive rotations about the coordinate axes.

1. DE 102 to 1950.0 FK 4

The most recent (1981) JPL ephemeris is DE 118 which is observationally adjusted to the FK 4 equinox at B 1950.0 ($\pm 0''.05$). One may approximately align DE 102 with the FK 4 at B 1950.0 by adjusting it to DE 118 at this epoch. The following rotation was determined by comparing the coordinates of the Earth-Moon barycenter at B 1950.0:

$$[\boldsymbol{r}, \dot{\boldsymbol{r}}]_{1950.0\,\mathrm{FK4}} \cong [\boldsymbol{r}, \dot{\boldsymbol{r}}]_{\mathrm{DE118}} = \boldsymbol{R}_x(-0''.00029)\,\boldsymbol{R}_y(-0''.11718)\,\boldsymbol{R}_z(+0''.66583)\,[\boldsymbol{r}, \dot{\boldsymbol{r}}]_{\mathrm{DE102}}$$

$$= \begin{bmatrix} 0.9999999999946285 & 0.0000032280349329 & 0.0000005681046715 \\ -0.0000032280349321 & 0.9999999999947899 & -0.0000000014059587 \\ -0.0000005681046761 & 0.0000000014041258 & 0.9999999999998386 \end{bmatrix} [\boldsymbol{r}, \dot{\boldsymbol{r}}]_{\mathrm{DE102}}$$

$\boldsymbol{R}(\alpha)$ indicates a rotation about the designated axis through the angle α.

2. DE 102 to 1950.0 dynamical equinox

The offset of DE 118 from the dynamical equinox at 1950.0 has been determined by Standish (1982) to be $E_{118}^{(\mathrm{R})}(1950.0) = +0''.53155$. One may combine this rotation with that above, a process which will preserve the 1950 obliquity as determined by DE 118:

$$[\boldsymbol{r}, \dot{\boldsymbol{r}}]_{1950.0\,\mathrm{DYN}} = \boldsymbol{R}_z(-0''.53155)\,[\boldsymbol{r}, \dot{\boldsymbol{r}}]_{\mathrm{DE118}}$$

$$= \begin{bmatrix} 0.9999999999966795 & -0.0000025770271219 & 0.0000000000000000 \\ 0.0000025770271219 & 0.9999999999966795 & 0.0000000000000000 \\ 0.0000000000000000 & 0.0000000000000000 & 1.0000000000000000 \end{bmatrix} [\boldsymbol{r}, \dot{\boldsymbol{r}}]_{\mathrm{DE118}}$$

$$= \begin{bmatrix} 0.9999999999996267 & 0.0000006510078110 & 0.0000005681046751 \\ -0.0000006510078102 & 0.9999999999997881 & -0.0000000014044957 \\ -0.0000005681046761 & 0.0000000014041258 & 0.9999999999998386 \end{bmatrix} [\boldsymbol{r}, \dot{\boldsymbol{r}}]_{\mathrm{DE102}}.$$

Note: The above offset from the dynamical equinox is defined in the "rotating" sense (see Standish, 1981) which is compatible with traditional usage. For the "inertial" sense of the definition, one has $E^{(I)}_{118} = +0''.62518$.

The above offset from the dynamical equinox of DE 118 was actually determined from an analysis of DE 102 spanning an interval of more than 1400 yr (Standish, 1982). This gave $E^{(I)}_{102}(1950.0) = +0''.22955$, and correspondingly $E^{(R)}_{102}(1950.0) = +0''.13591$. One relates these to the corresponding values for DE 118 by the formula $\Delta E = \theta_z + \theta_y \operatorname{ctn}\bar{\varepsilon}$, where the θ's are the rotational angles relating the two ephemerides and $\bar{\varepsilon}$ denotes the mean obliquity.

Also found in the analysis is the value of the mean obliquity, $\bar{\varepsilon}^{(I)}_{102}(1950.0) = 23°26'44''.813$ and, correspondingly, $\bar{\varepsilon}^{(R)}_{102}(1950.0) = 23°26'44''.816$. This latter number should represent a significant improvement ($\pm 0''.015$) over the 1976 IAU value evaluated at 1950.0 of $23°26'44''.855$ (Lieske et al., 1977). The value for DE 118 supports the DE 102 value since $\bar{\varepsilon}_{118} - \bar{\varepsilon}_{102} = -\theta_x = +0''.00029$, and the expected obliquity error for DE 118 is half that of DE 102. A similar value for DE 102 was found by Bretagnon and Chapront (1981).

The rotation angle $\theta_y = -0.11718$ is almost entirely due to the difference between the old and new precession constants ($1''.1\ \mathrm{cy}^{-1}$) over the interval 1974 to 1950.0. The reduction of the lunar data in DE 102 used the old precession constant (see Sect. VII.C) while the lunar data were reduced in DE 118 using the new value ($\theta_y \approx 1.1 \times 0.24 \sin\varepsilon$).

3. DE 102 to 2000 dynamical equinox

One may further transform to the J 2000 system by using the matrix (Standish, 1982) which was actually used to create DE 200 from DE 118. This is

$$[r, \dot{r}]_{2000\mathrm{DYN}} = \begin{bmatrix} 0.9999256791774783 & -0.0111815116768724 & -0.0048590038154553 \\ 0.0111815116959975 & 0.9999374845751042 & -0.0000271625775175 \\ 0.0048590037714450 & -0.0000271704492210 & 0.9999881946023742 \end{bmatrix} [r, \dot{r}]_{\mathrm{DE118}}$$

$$= \begin{bmatrix} 0.9999257180268403 & -0.0111782838886141 & -0.0048584357372842 \\ 0.0111782838782385 & 0.9999375206641666 & -0.0000271576311202 \\ 0.0048584357611567 & -0.0000271533600777 & 0.9999881973626738 \end{bmatrix} [r, \dot{r}]_{\mathrm{DE102}}.$$

While the above matrices do align the Earth-Moon barycenter coordinates to those of DE 118 at 1950.0, they will be less precise for any other body or any other time due to the differences in the orbital motions between the two ephemerides. For more precise approximations to each body over extended periods of time, the formulation of Sect. VIII.B is recommended.

B. Orbital improvements

One may quite closely approximate DE 118 by using the positions and velocities of DE 102 and by modifying these using the Set III formulation of Brouwer and Clemence (1961, p. 241). The corrections to the elements have been determined by matching DE 102 to DE 118 over two hundred years (1850–2050) and then by fitting these corrections with quadratic polynomials in time. For the Moon, two pairs of trigonometric terms were added with periods of the node and perigee precession (18.6 and 8.85 yr). In using these expressions, one must use $t = 0$ in the Set III formulation; we have found this to be more accurate than the Keplerian assumption of constant elements referred to a single epoch. Table 7 gives the Set III element corrections for each body in units of arc s; for use with the formulas, they should be divided by 206,265. The corrections are applied using

$$r_{\mathrm{DE118}} = \left[\frac{\partial r_{\mathrm{DE102}}}{\partial S_{\mathrm{III}}}\right] \Delta S_{\mathrm{III}} + r_{\mathrm{DE102}},$$

where the partial derivatives are given in Brouwer and Clemence (1961, p. 241), using $t = 0$ in the matrix, using osculating Keplerian elements at each time point, and using the definitions on pages 35 and 237.

Caution: Because of the coarse-grained representation of Mercury's coordinates in DE 102 (see Sect. IV), this process will work accurately for Mercury only at the mesh points of the Chebyshev polynomials; i.e., only at times for which JED-2440400.5 = 8*k*, where *k* is an integer.

The differences in Table 7 illustrate the discussion of orbit accuracies (VII.D). The mean motions of the inner three planets

Table 7. Set III corrections for DE 118–DE 102, with
T = (JED-2433282.5)/36525,
$A = 2\pi\ 36525/6798.36$, and $B = 2\pi\ 36525/3231.48$

		$\Delta\epsilon_0 + \Delta r$	Δp	Δq	$e\Delta r$	$\Delta a/a$	Δe
MERCURY	1	-.63997	-.18676	-.10567	-.13231	.00000	-.00020
	T	-.03330	-.00049	.00056	.00020	.00000	.00000
	T**2	.00010	.00002	-.00001	.00000	.00000	.00000
VENUS	1	-.65261	-.15210	.08000	-.00422	.00000	.00033
	T	-.04294	-.00026	.00000	.00005	.00000	.00000
	T**2	.00022	.00000	.00000	.00000	.00000	.00000
E-M BARY	1	-.65706	-.15399	.03259	-.01080	.00000	.00013
	T	-.03791	.00034	.00093	.00008	.00000	-.00007
	T**2	.00036	.00000	.00000	.00000	.00000	.00000
MARS	1	-.66103	.08275	-.14208	-.06178	.00000	.00000
	T	-.00664	-.00101	-.00087	.00073	.00000	.00019
	T**2	.00000	.00000	.00007	.00000	.00000	.00000
JUPITER	1	-.67338	-.02460	-.15128	-.04013	.00559	.02466
	T	-.39304	-.00143	-.00070	.00000	.00000	.00000
	T**2	.00000	.00000	.00000	.00000	.00000	.00000
SATURN	1	-.68056	-.08530	.06382	-.05454	.02418	.00000
	T	-.19254	-.00252	-.00388	-.05626	.00000	.00000
	T**2	.04676	.00242	-.00316	.03115	.00000	.00000
URANUS	1	-.60940	.04462	.10435	.00000	.00000	.01286
	T	-.37558	-.04178	-.01306	.19064	.03943	.00000
	T**2	-.24203	-.02195	-.00958	.14047	.03814	.05512
NEPTUNE	1	-.52662	-.05354	-.10839	-.26007	-.52933	.31788
	T	2.70019	.03764	.01100	.29747	.04393	-.14760
	T**2	-1.11469	-.03502	-.03346	-.11951	-.14544	-.19803
PLUTO	1	.31296	-.14721	.32918	.09530	-.59697	.55239
	T	1.53554	.01414	-.00774	.00000	-.06691	-.14922
	T**2	.00000	.00000	.00890	-.11620	.12534	.14817
THE MOON	1	-.57722	.00000	.00000	-.03745	-.01621	.00000
	T	-.62624	.00000	.00000	.00000	.00000	.00000
	T**2	1.18544	.00000	.00000	.00000	.00000	.00000
	COS(A*T)	.01289	.00000	.00000	.00000	.00000	.00000
	SIN(A*T)	.00000	.00000	.00000	.00000	.00000	.00000
	COS(B*T)	.00000	.07427	.14255	.00000	.00000	.00000
	SIN(B*T)	.00000	.13866	-.07364	.00000	.00000	.00000

shift together, because the radar data determine the differences better than they do the inertial rates. The differential and inertial mean motion shifts for Earth and Mars result from two mass differences in the two ephemerides. The change in Jupiter's mass introduces a short-period (1.12 yr) periodicity in Mars' longitude. The Mariner 9 and Viking data blocks occur four cycles apart and are nearly centered on the phase of maximum rate. The rate change averages about $0''.03\,cy^{-1}$ over each block separately. A 15% change in Vesta's mass causes a long period change of $0''.007\,cy^{-1}$.

It is reassuring that the $1''.185\,cy^{-2}$ coefficient of T^2 for the Moon's element $\Delta\ell_0+\Delta r$ compares well with the $1''.20\,cy^{-2}$ difference expected from the change in the Love number and phase angle.

The improvements resulting from the above adjustments are discussed in the following section.

IX. Comparison of DE 102 with DE 118

At the present time, DE 118 represents JPL's best ephemeris. One may get an idea of how well DE 102 approximates DE 118 by comparing the two at a number of time points covering the interval 1850–2050.

The most obvious difference between DE 102 and DE 118, during the present century at least, is the difference in the orientation of axes as discussed in Sect. VIII.A.1. This rotation produces signatures in the heliocentric coordinates of the form

$$\Delta\alpha(102\text{–}118)\cong+0''.67+0''.12\sin\alpha\tan\delta$$

and

$$\Delta\delta(102\text{–}118)\cong+0''.12\cos\alpha.$$

Superposed on these signatures, however, are other trends due to the orbital adjustments of each body.

One may compare the ephemerides after the rotation of Sect. VIII.A.1 is applied. The improvement is remarkable for the 4 innermost planets. However, secular trends in α remain, up to $0''.05\,cy.^{-1}$. The 5 outer planets show only slight improvement. For the Moon, the quadratic term of $1''.2\,cy^{-2}$ is in evidence. Table 8a gives the maximum deviation for each body in heliocentric coordinates for this comparison over the time 1850–2050.

One may also compare DE 118 with DE 102 after the Set III corrections of Sect. VIII.B have been applied. The inner planets show remarkable agreement (better than 0".001); and the discrepancy between the values of the Moon's secular acceleration has disappeared. Table 8b gives the corresponding maximum deviations for these comparisons. The four inner planets and the Moon show no further evidence of secular trends. The outer planets are less well fit by this process and still exhibit evidence of impending run-off, possibly due to the fact that the masses of these bodies have changed between the ephemerides, therefore weakening the validity of the Set III formulation. Unquestionably the differences between the two ephemerides could be further improved for the outer planets and Moon by fitting analytical theories in place of Set III parameters. The changes in masses and perturbations would then be accommodated.

These statements have been supported by a further comparison. DE 118 was integrated backward another 50 yr to 1800, the Set III adjustments were applied to DE 102 over this time period, and the comparison was made over this "extrapolated" interval. The statements above remain valid.

Table 8a. Maximum deviations in heliocentric coordinates over the interval 1850–2050 between DE 118 and DE 102 after the application of the rotation in Sect. VIII.A.1

	$\lvert\Delta\alpha\rvert_{max}$	$\lvert\Delta\delta\rvert_{max}$	$\lvert\Delta\varrho\rvert_{max}$
Mercury	0".05	0".02	2.2 km
Venus	0.05	0.02	0.4
$E-M$ Barycenter	0.04	0.02	0.7
Mars	0.02	0.02	1.6
Jupiter	0.5	0.16	150
Saturn	0.3	0.16	600
Uranus	1.2	0.50	5,000
Neptune	3.6	1.3	15,000
Pluto	4.0	1.2	30,000
Geocentric Moon	2.0	0.8	0.3

Table 8b. Maximum deviations in heliocentric coordinates over the interval 1850–2050 between DE 118 and DE 102 after the application of the Set III corrections given in Sect. VIII.B

	$\lvert\Delta\alpha\rvert_{max}$	$\lvert\Delta\delta\rvert_{max}$	$\lvert\Delta\varrho\rvert_{max}$
Mercury	0".0002	0".0001	0.03 km
Venus	0.0003	0.0003	0.05
$E-M$ Barycenter	0.0003	0.0005	0.09
Mars	0.0020	0.0006	0.8
Jupiter	0.10	0.03	120
Saturn	0.15	0.05	400
Uranus	0.25	0.07	1100
Neptune	0.60	0.25	7000
Pluto	0.20	0.05	7000
Geocentric Moon	0.04	0.11	0.05

X. DE 102 export tapes

In the past five years, JPL has released for export more than 100 copies of its various ephemerides to users throughout the world. We now have the capability of providing direct, machine-readable, nonformatted tapes for a number of different types of computers including IBM, Modcomp, CDC Cyber, PDP 11, VAX, Honeywell, and UNIVAC. We also provide reading and interpolating software, character-coded in Field data, BCD, ASC II, or EBCDIC.

All 44 centuries of DE 102 can be written onto two 2400 ft magnetic tapes at a density of 6250 bpi. Users wishing a copy are asked to contact E. M. Standish; JPL, 264–664; Pasadena, CA 91109, USA.

XI. Conclusion

The 44-cy span of DE 102 makes it an ideal test for analytical theories of the planets and Moon. The published comparisons are listed in the Introduction. Given the long span either the analytical comparisons or Fourier analysis (Standish, 1982) can be used to recover the obliquity and equinox offset which are implicit in the data fits and integration. These are parameters fundamental to accurate coordinate systems. We find an obliquity $0''.039\pm0''.015$

smaller than the recently adopted (1976) IAU value. The long span should also prove useful for comparison with historical observations. The improved parameters from the planetary fits are given in Table 4. Notable among these is the AU = 149597870.68 ± 0.03 km. The lunar ephemeris (LE 51) in DE 102 has been used for lunar laser predictions for the past several years. Though the accuracy of DE 102 has been superseded by subsequent ephemerides, its length will give it unique value for some years to come.

Acknowledgements. We particularly wish to thank P. M. Muller who suggested the project for the long integration. T. C. Van Flandern has encouraged us from the start and worked in parallel with his fits. W. S. Sinclair aided in the lunar data analysis; M. S. W. Keesey aided in the planetary data analysis. The research described in this paper was carried out by the Jet Propulsion Laboratory, California Institute of Technology, under contract with the National Aeronautics and Space Administration.

References

Abbot, R.I., Shelus, P.J., Mulholland, J.D., Silverberg, E.C.: 1973, *Astron. J.* **78**, 784

Bretagnon, P., Chapront, J.: 1981, *Astron. Astrophys.* **103**, 103

Brouwer, D., Clemence, G.M.: 1961, Methods of Celestial Mechanics, Academic Press, New York

Calame, O., Mulholland, J.D.: 1978a, *Science* **199**, 977

Calame, O., Mulholland, J.D.: 1978b, in *Tidal Friction and the Earth's Rotation*, ed. P. Brosche and J. Sunderman, Springer, New York, p. 43

Cappallo, R.J.: 1980, The Rotation of the Moon, Ph. D. Thesis, Mass. Inst. of Techn., Cambridge

Cappallo, R.J., King, R.W., Counselman, C.C., III, Shapiro, I.I.: 1981, *Moon and Planets* **24**, 281

Chapront, J., Chapront-Touzé, M.: 1981, *Astron. Astrophys.* **103**, 295

Chapront, J., Chapront-Touzé, M.: 1982, in *High-Precision Earth Rotation and Earth-Moon Dynamics: Lunar Distances and Related Observations*, O. Calame, ed., Reidel, Dordrecht, p. 257

Chapront, J., Chapront-Touzé, M.: 1983, *Astron. Astrophys.* (in press)

Chapront-Touzé, M.: 1983, *Astron. Astrophys.* **119**, 256

Chapront-Touzé, M., Chapront, J.: 1980, *Astron. Astrophys.* **91**, 233

Cohen, C.J., Hubbard, E.C., Oesterwinter, C.: 1967, *Astron. J.* **72**, 973

Dickey, J.O., Williams, J.G., Yoder, C.F.: 1982, in *Proc.* IAU *Coll.* **63**, High-Precision Earth Rotation and Earth-Moon Dynamics: Lunar Distances and Related Observations, O. Calame, ed., Reidel, Dordrecht, p. 209

Dickey, J.O., Williams, J.G.: 1982, Geophysical Applications of Lunar Laser Ranging, *EOS* **63**, 301

Dunham, D.W., Sofia, S., Fiala, A.D., Herald, D., Muller, P.M.: 1980, *Science* **210**, 1243

Eckhardt, D.H.: 1967, in *Measure of the Moon*, eds. Z. Kopal and C.L. Goudas, D. Reidel, Dordrecht, p. 40–51

Eckhardt, D.H.: 1972, *Moon* **6**, 127

Eckhardt, D.H.: 1981, *Moon Planets* **25**, 3

Eckhardt, D.H.: 1982, in *Proc.* IAU *Coll.* **63**, *High-Precision Earth Rotation and Earth-Moon Dynamics. Lunar Distances and Related Observations*, O. Calame, ed., Reidel, Dordrecht, p. 193

Estabrook, F.B.: 1971, Derivation of Relativistic Lagrangian for *n*-Body Equations Containing Relativity Parameters β and γ, JPL Internal Communication

Ferrari, A.J., Sinclair, W.S., Sjogren, W.L., Williams, J.G., Yoder, C.F.: 1980, *J. Geophys. Res.* **85**, 3939

Fricke, W.: 1968, *Mitt. Astron. Rechen-Inst. Heidelberg*, Serie B, No. 16

Fricke, W.: 1982, *Astron. Astrophys.* **107**, L 13

Gaposchkin, E.M.: 1974, *J. Geophys. Res.* **79**, 5377

Gaposchkin, E.M. (Ed.): 1973, *Smithsonian Astrophys. Obs. Spec. Rept.* **353**, 388pp.

Goldstein, H.: 1950, Classical Mechanics, Addison-Wesley, Reading, Mass.

Henrard, J.: 1980, *Celes. Mech.* **22**, 335

Hertz, H.G.: 1968, *Science* **160**, 299

Jordan, J.F., Melbourne, W.G., Anderson, J.D.: 1972, Testing Relativistic Gravity Theories Using Radio Tracking Data from Planetary Orbiting Spacecraft, Paper at 15th Planetary Meeting of Cospar, Madrid

Kaula, W.M., Baxa, P.A.: 1973, *Moon* **8**, 287

Kaula, W.M.: 1966, Theory of Satellite Geodesy, Blaisdell Publ. Co., Mass.

Krogh, F.T.: 1972, in *Lecture Notes in Mathematics* **362**, 22, Springer-Verlag, New York

Lestrade, J.-F.: 1981, *Astron. Astrophys.* **100**, 143

Lestrade, J.-F., Bretagnon, P.: 1982, *Astron. Astrophys.* **105**, 42

Lieske, J.H., Lederle, T., Fricke, W., Morando, B.: 1977, *Astron. Astrophys.* **58**, 1

Martin, C.F., Van Flandern, T.C.: 1970, *Science* **168**, 246

Migus, A.: 1980, *Moon and Planets* **23**, 391

Moons, M.: 1981, *Celes. Mech.* **26**, 131

Morrison, L.V., Ward, C.G.: 1975, *Monthly Notices Roy. Astron. Soc.* **173**, 183

Moyer, T.D.: 1971, Jet Propulsion Laboratory Tech. Rept. 32–1527, Pasadena

Moyer, T.D.: 1981a, *Celes. Mech.* **23**, 33

Moyer, T.D.: 1981b, *Celes. Mech.* **23**, 57

Muhleman, D.O., Esposito, P.B., Anderson, J.D.: 1977, *Astrophys. J.* **211**, 943

Mulholland, J.D., Shelus, P.J., Silverberg, E.C.: 1975, *Astron. J.* **80**, 1087

Muller, P.M.: 1975, An Analysis of the Ancient Astronomical Observations with the Implications for Geophysics and Cosmology, Thesis, Univ. Newcastle upon Tyne, School of Physics, Fiddes Litho Press

Muller, P.M., Stephenson, F.R.: 1975, The Acceleration of the Earth and Moon from Early Astronomical Observations, in *Growth Rhythms and History of the Earth's Rotation*, Eds. Rosenberg, G.D., Runcorn, S., K., John Wiley, London

Null, G.W.: 1970, *Bull. Am. Astron. Soc.* **2**, 251

Oesterwinter, C., Cohen, C.J.: 1972, *Celes. Mech.* **5**, 317

O'Handley, D.A., Holdridge, D.B., Melbourne, W.G., Mulholland, J.D.: 1969, *Jet Propulsion Laboratory Tech. Rept.* 32–1465

Shapiro, I.I.: 1980, *Science* **208**, 51

Shapiro, I.I., Counselman, C.C., III, King, R.W.: 1976, *Phys. Rev. Letters* **36**, 555

Shapiro, I.I.: 1964, *Phys. Rev. Letters* **13**, 789

Shelus, P.J., Mulholland, J.D., Silverberg, E.C.: 1975, *Astron. J.* **80**, 154

Schubart, J.: 1974, *Astron. Astrophys.* **30**, 289

Smart, W.N.: 1931, Spherical Astronomy, Cambridge Univ. Press

Standaert, D.: 1980, *Celes. Mech.* **22**, 357

Standish, E.M.: 1973, *Astron. Astrophys.* **26**, 463

Standish, E.M.: 1981, *Astron. Astrophys.* **101**, L 17
Standish, E.M.: 1982, *Astron. Astrophys.* **114**, 297
Standish, E.M., Keesey, M.S.W., Newhall, X X: 1976, *Jet Propulsion Laboratory Tech. Rept.* 32–1603
Stephenson, F.R., Houlden, M.A.: 1981, *J. Hist. Astron.* **12**, 133
Stumpff, P.: 1981, *Astron. Astrophys.* **101**, 52
Van Flandern, T.C.: 1982, Improved Mean Elements for the Earth and Moon (private communication)
Van Flandern, T.C.: 1975, *Monthly Notices Roy. Astron. Soc.* **170**, 333
Will, C.M.: 1974, in *Experimental Gravitation*, B. Bertotti, Ed., Academic Press
Williams, J.G.: 1984 (in press)
Williams, J.G.: 1977, in *Scientific Applications of Lunar Laser Ranging*, ed. J. D. Mulholland, D. Reidel, Hingham, Mass., p. 37
Williams, J.G., Sinclair, W.S., Yoder, C.F.: 1978, *Geophys. Res. Letters* **5**, 943
Williams, J.G., Dicke, R.H., Bender, P.L., Alley, C.O., Carter, W.E., Currie, D.G., Eckhardt, D.H., Faller, J.E., Kaula, W.M., Mulholland, J.D., Plotkin, H.H., Poultney, S.K., Shelus, P.J., Silverberg, E.C., Sinclair, W.S., Slade, M.A., Wilkinson, D.T.: 1976, *Phys. Rev. Letters* **36**, 551
Williams, J.G., Slade, M.A., Eckhardt, D.H., Kaula, W.M.: 1973, *Moon* **8**, 469
Williams, J.G., Melbourne, W.G.: 1982, in *Proc.* IAU *Coll.* **63**, *High Precision Earth Rotation and Earth-Moon Dynamics; Lunar Distances and Related Observations*, O. Calame, ed., Reidel, Dordrecht, 293–303
Wong, S.K., Reinbold, S.J.: 1973, *Nature* **241**, 111
Yoder, C.F.: 1979, in *Natural and Artificial Satellite Motion*, ed. P. Nacozy and S. Ferrez-Mello, Univ. Texas Press, Austin, p. 211